Posted on 30 Nov 2022 — The copyright holder is the author/funder. All rights reserved. No reuse without permission. — https://doi.org/10.1002/essoar.10505921/v1 — This a preprint and has not been peer reviewed. Data may be preliminary.

Trophic state assessment of a freshwater Himalayan lake using Landsat 8 OLI satellite Landsat 8 OLI, Secchi disk depth (Z SD), Trophic State Index (TSI)

Fayma Mushtaq[1], mili lala[2], and Afaan Gulzar Mantoo[1]

[1]Department of Ecology, Environment & Remote Sensing
[2]Birla Institute of Technology

November 30, 2022

Abstract

3 A new version of Trophic State Index for freshwater Himalayan lake (TSI FHL) has been 4 derived from Landsat 8 OLI to determine the aquatic health of the lake ecosystem. TSI FHL is 5 based on chlorophyll-a concentration (C Chl-a) which has been retrieved from Landsat 8 OLI 6 data and laboratory measurements using an empirical approach. Further, in-situ 7 measurements have also been taken with Secchi disk depth (Z SD) in a freshwater Himalayan 8 lake (FHL). The derived C Chl-a exhibited lower and upper limit of 25.81 µg/L and 207.96 9 µg/L respectively. The modelled Z SD values ranged between 0.18 m to 0.66 m with an 10 average depth of 0.50 m. The best-fitted regression model, developed for C Chl-a with R^2 = 11 0.89, exhibited model error of 0.77 µg/L for the Standard Error of Estimate (SEE). The Mean 12 Absolute Percentage Error (MAPE) and Nash-Sutcliffe coefficient (E) values were 5.83 % 13 and 0.98 µg/L respectively. For the Z SD, the best-fitted model showed errors of 0.11 µg/L 14 (SEE), 13.93 % (MAPE), and 0.77 µg/L (E) with R^2 = 0.84. 15

Trophic state assessment of a freshwater Himalayan lake using Landsat 8 OLI satellite imagery: A case study of Wular Lake

Abstract

A new version of Trophic State Index for freshwater Himalayan lake (TSI_{FHL}) has been derived from Landsat 8 OLI to determine the aquatic health of the lake ecosystem. TSI_{FHL} is based on chlorophyll-a concentration ($C_{Chl\text{-}a}$) which has been retrieved from Landsat 8 OLI data and laboratory measurements using an empirical approach. Further, in-situ measurements have also been taken with Secchi disk depth (Z_{SD}) in a freshwater Himalayan lake (FHL). The derived $C_{Chl\text{-}a}$ exhibited lower and upper limit of 25.81 µg/L and 207.96 µg/L respectively. The modelled Z_{SD} values ranged between 0.18 m to 0.66 m with an average depth of 0.50 m. The best-fitted regression model, developed for $C_{Chl\text{-}a}$ with R^2 = 0.89, exhibited model error of 0.77 µg/L for the Standard Error of Estimate (SEE). The Mean Absolute Percentage Error (MAPE) and Nash–Sutcliffe coefficient (E) values were 5.83 % and 0.98 µg/L respectively. For the $Z_{SD,}$ the best-fitted model showed errors of 0.11 µg/L (SEE), 13.93 % (MAPE), and 0.77 µg/L (E) with R^2 = 0.84.

Keywords: Chlorophyll-a Concentration ($C_{Chl\text{-}a}$), Eutrophication, Himalayan Lake, Landsat 8 OLI, Secchi disk depth (Z_{SD}), Trophic State Index (TSI)

1. Introduction

Freshwater ecosystems across the globe are under substantial stress and prone to frequent manifestations such as harmful algal blooms (Lee et al., 2016) which pose threat to society and environment restricting lives of humans and animals dependent on lake ecosystem (Le et al., 2013; Smith, 2006). Being the primary source of organic carbon, biogeochemical process and base of aquatic food web, phytoplankton has a significant impact on lake ecosystem and water quality (French & Petticrew, 2007; Palmer et al., 2015; Williamson et al., 2009; Zheng & DiGiacomo, 2017). For a biologically productive and healthy lake, the concentration of phytoplankton and algae should be under optimal concentration (Patra et al., 2017). The disproportionate growth of the phytoplankton biomass resulting from anthropogenic nutrient enrichment can lead to trophic level failure, shifts in species diversity, disappearance of benthic fauna at several trophic levels (Glibert et al., 2002; Paerl & Paul, 2012; Vadeboncoeur et al., 2003).

Although, the process of lake eutrophication is natural but recent studies have revealed that it could accelerate in response to the effects of anthropogenic events and or climate change (Li et al., 2011; Watanabe et al., 2015). The excessive growth in plants due to

enrichment of nutrients and minerals by anthropogenic activities also termed as Cultural eutrophication, results in lake's ecological imbalance, increased turbidity and loss of submerged macrophytes (Yu et al., 2015). The critical level of eutrophication includes hypoxia (dearth of oxygen) and noxious algal blooms which leads to severe damage to aquatic life like massive fish mortality (Dua et al., 2019; Wen et al., 2018). Recently, large number of lakes are suffering from recurrent algal blooms and this phenomenon has turned out to be a global environmental problem (Chen et al., 2017; Wang & Liang, 2015). Therefore, it is important to monitor phytoplankton biomass in lake ecosystems. The estimation of Chlorophyll-a (Chl-a) for evaluation of the trophic status of aquatic system is effective for scrutinizing and managing eutrophic lakes (Carlson, 1977).

In water bodies, profusion of phytoplankton biomass is usually measured with a proxy i.e. by quantifying the concentration of chlorophyll-a ($C_{Chl\text{-}a}$), which determines the water quality and biophysical status (Huot et al., 2007; Moses et al., 2009). Besides, $C_{Chl\text{-}a}$ is considered as an indicator of eutrophication which indicates about the ecological health of aquatic environment and water trophic level (Ha et al., 2017; Kasprzak et al., 2008; Yang et al., 2010). The conventional methods of Chl-a measurement involve estimation of its concentration spectrophotometrically after the collection and preservation of water samples (Chen et al., 2013). The other methods involve in situ measurements with chlorophyll fluorometers and remotely with optical radiometers (Dickey et al., 2006). Nevertheless, these methods are not well suited as they limit investigators to represent a synoptic Spatio-temporal view of a waterbody (Chen et al., 2011; Giardino et al., 2001; Lim & Choi, 2015). Satellite remote sensing has been extensively used for monitoring and managing water quality (Bukata, 2013; Guo et al., 2016; Mushtaq & Nee Lala, 2017a) due to its potential to provide consistent Spatio-temporal observations at a large scale (Han et al., 2014; Senay & Shafique, 2001). The assessment of Chl-a using geospatial technique is a well-recognized scientific application (Schalles, 2006), generally based on empirical relationships between the sensor reflectance and Chl-a (Ritchie et al., 2003). Numerous studies have been conducted globally and algorithms have been developed for mapping and monitoring of $C_{Chl\text{-}a}$ and trophic state using various satellite data (Bresciani et al., 2018; Cunha et al., 2013; Gurlin et al., 2011; X. Li et al., 2017; Yang et al., 2010).

The present study is a preliminary contribution to bio-optical research based on properties of Chlorophyll-a (Chl-a) and Secchi Disk Depth (Z_{SD}) using geospatial techniques of one of the largest freshwater lakes in Asia sited in Kashmir Himalayas. The study lays a

theoretical foundation for further research on this lake ecosystem in near future. In the present study, the performance, and applicability of multiband ratio algorithm for estimation of $C_{Chl\text{-}a}$ and Z_{SD} in a freshwater Himalayan lake (FHL) in Kashmir Himalayas has been investigated. Furthermore, to determine the aquatic health of lake ecosystem a new version of Trophic State Index (TSI) for a freshwater Himalayan lake (TSI_{FHL}) has been derived from Landsat 8 OLI.

2. Study area and test sites

The Wular lake is one of the largest freshwater lakes of Asia, located in the north-west of Kashmir Himalayas (34°16' - 34°32' N latitude and 74°28' - 74°48' E longitude), ~55 km from Srinagar city at an altitude of 1,580 m (a.m.s.l) (Fig. 1). The river "Jhelum", "Madhumati", and "Erin" are the vital sources of inflow into Wular lake, with only single outlet in the form of River Jhelum in south-west (near Sopore). According to the reports of (National Wetland Atlas 2010) the lake is elliptical in shape, formed by meandering of River Jhelum with maximum length of 16 km (North to South) and width of 9.6 km (East to West). The depth measurement confirms that the lake is optically shallow (average ~1 m). The lake is of paramount importance because of its ecologically rich environment and is designated as Wetland of International Importance under Ramsar Convention-1990. It serves as a significant habitat for migratory waterbirds (like ducks, shorebirds, geese, and cranes), major fisheries resource (Schizothorax niger, Triplophisa marmorata and Triplophysa kashmirensis), source of plant species (Trapa and Nelumbium nucifera) in Kashmir Valley (Wetlands International 2007). The area falls in a temperate climate zone with four distinct seasons: spring, summer, autumn, and winter (Jeelani et al., 2012). The dominant amount of precipitation falls during winter and spring months from westerlies, while summer and autumn are comparatively drier (Mushtaq et al., 2020). According to the report of Wetland International (2007), the maximum discharge occurs during May and June with the maximum peaks exceeding 1500 cumecs. A moderate mean discharge of above 1000 cumecs occurs during August and the discharges lower down in the lean seasons in Wular lake particularly during late October to February.

3. Materials and methods

3.1. Field measurements and laboratory analysis

The present study was prearranged and carried out in the month of October taking into consideration possible dates of satellite overpass (October 7, 2018) and minimun contribution

of heavy runoff and sediment load into the Wular lake. The water samples (n = 20) were collected during October 4 - 5, 2018 at depth of approximately (0.3 - 0.4 m) in 1 Litre polyethylene bottles from the open water portion distributed along the North - western to southern fringe of Wular lake (Fig. 1). A black-and-white disk with a diameter of ~ 20 cm was used to measure the Z_{SD} at each sampling site and sample locations were concurrently recorded using hand-held Trimble GPS receiver. Prior to spectrophotometric analysis, the water samples were filtered on Whatman GF/C filter paper and stored at (- 20° C) followed by extraction of Chl-a with methanol using centrifugation for 10 min at 4000 rpm in centrifuge machine. The $C_{Chl\text{-}a}$ were measured by spectrophotometer at 750 and 665 nm (Holm-Hansen & Riemann, 2006; Lorenzen, 1967; Talling et al., 1980) (Table 1).

3.2. Landsat 8 OLI image acquisition and pre-processing

The cloud-free Landsat 8 OLI Level 1T image (Scene-ID:LC81490362018280LGN00; path: 149 and row: 36) of October 07, 2018 was obtained from USGS Earth Explorer data portal to develop Chl-a and Z_{SD} algorithm which was further incorporated in the assessment of TSI_{FHL}. Landsat data is ideal for wide range of application in domain of water quality due to 30 m spatial resolution which allows synoptic observation of lakes (Lee et al., 2016). Ma & Dai (2005) confirmed about the effective applicability of Landsat sensor data and field spectral measurement for study of chlorophyll-a and total suspended matter concentrations in Taihu Lake, China. The scene used in this study was already corrected for geometrical errors, atmospheric perturbations were rectified by means of dark object subtraction (DOS) method using the radiometric rescaling coefficients (Chávez, 1996) and the digital numbers (DNs) were converted to water reflectance (Lu et al., 2002; Yang & Lo, 2000). The true spectral reflectance (ρw) of water was calculated by the equation as follows:

$$\rho w = (Lsat_{rad} - Lhaze1\%_{rad})\pi \times \frac{d^2}{Eo\lambda} \times \cos\theta s \times TAU_v \qquad (1)$$

where, ρw is the spectral reflectance of water, $Lsat_{rad}$ and *L*haze denotes the radiances at sensor and atmospheric path, respectively, d is distance between earth and sun (in astronomical units), $Eo\lambda$ is exo-atmospheric solar irradiance, θ is sun zenith angle, TAU_v is atmospheric transmittance along the path from the ground surface to the sensor. Based on Normalized difference water index (NDWI) (McFeeters, 1996), the North-eastern part of the lake was excluded from the analysis as the area is characterized by highly dense aquatic vegetation.

3.3. Algorithm development and model calibration for $C_{Chl\text{-}a}$ and Z_{SD}

For the development of analytical models of biophysical parameters ($C_{Chl\text{-}a}$ and Z_{SD}) for FHL, different set of regression models (linear and nonlinear) have been explored using various band combinations of Landsat 8 OLI. The most ideal method for estimation of Chl-a using Geospatial technique is the implementation of empirical relationship between $C_{Chl\text{-}a}$ and sensor reflectance (Bohn et al., 2018; Haung et al., 2010; Matus-Hernandez et al., 2018; Mayo et al., 1995; Murugan et al., 2014; Salem et al., 2017). For the development of regression model, the total samples (n = 20) were distributed into two sets: one set for regression modelling i.e. 80% (n = 16) while as other set for validation of model i.e. 20% (n = 4). The best retrieval model was investigated empirically by formulating a regression algorithm for each single band as well as multiple bands to select the one with highest (R^2). In case of Z_{SD} reciprocal reflectance have been used in modelling process because it reduces the bidirectional and viewing geometrical difference properties (Singh et al., 2014). The empirical algorithm established from the single and multiband ratios for retrieval of Z_{SD} and $C_{Chl\text{-}a}$ can be expressed by Equation No. (2) & (3).

$$Z_{SD} = [a_1; \dots\dots\dots a_2;\ \rho w^{-1}(\lambda_1)] \qquad (2)$$

$$C_{Chl-a} = \left[a_1; \dots\dots\dots a_2; \frac{\{\rho w(\lambda_1) - \rho w(\lambda_2)\}}{\rho w(\lambda_3)}\right] \qquad (3)$$

where a_1 and a_2 are the regression coefficients: λ_1 = 865 nm (spectral region between 851 - 879 nm) is sensitive to the reflection caused by an interaction of algal-cell scattering and a minimum combined effect of pigment and water absorption (Rundquist et al., 1995). λ_2 = 482 nm (spectral region between 452 - 512 nm) is maximally sensitive to the absorption of blue light due to chlorophyll-a concentration. In case of clear water, the reflection in this region is approximately 2% which drops gradually to 1% at higher wavelengths. λ_3 = 561 nm (spectral region between 533 - 590 nm) is maximally sensitive to the reflectance caused by relatively lower absorption of green light by algae (Gitelson, 1992). The bands ratios were used in the development of model as the spectral band ratios are the more preferred because they help to reduce the irradiance, atmospheric and air-water surface effects on reflectance (Dekker et al., 1993; Lillesand et al., 2015).

3.4. Model evaluation and validation

To evaluate the efficacy and forecast precision of the best model based on reflectance measurement, validation was performed using the field samples. The algorithms performance and errors were computed using three statistic metrics including SEE (Standard error of estimate), E (Nash–Sutcliffe model efficiency coefficient), MAPE (Mean absolute percentage error) and Bias given below:

$$SEE = \sqrt{\sum_{i=1}^{n} \left(X_{meas,i} - X_{pred,i}\right)^2 \Big/ n} \quad (4)$$

$$MAPE = n^{-1} \sum_{i=1}^{n} \left| \frac{X_{meas,i} - X_{pred,i}}{BPP_{meas,i}} \right| \times 100 \quad (5)$$

$$E = 1 - \left[\frac{\sum_{i=1}^{n} \left(X_{meas,i} - X_{pred,i}\right)^2}{\sum_{i=1}^{n} \left(X_{meas,i} - \overline{X}_{meas,i}\right)^2} \right] \quad (6)$$

$$Bias = n^{-1} \sum_{i=1}^{n} \left(X_{meas,i} - X_{pred,i}\right) \quad (7)$$

where *n* represents number of samples, $X_{meas,i}$ and $X_{pred,i}$ represents the measured and predicted biophysical parameters ($C_{Chl\text{-}a}$ and Z_{SD}) of the i^{th} sample respectively.

3.5. Evaluation of TSI_{FHL}

To better understand the trophic status of freshwater Himalayan lake (FHL), a new version of TSI derived from Landsat 8 OLI has been proposed for freshwater Himalayan lake (TSI_{FHL}). Due to the unavailability of the total phosphorous data, the trophic state assessment was carried out on the basis of Z_{SD} and Chl-a. $C_{Chl\text{-}a}$ is recommended as a trophic status indicator since its values are not much altered due to other environmental factors (Carlson, 1977). For index generation, regression analysis was performed between in-situ data of Z_{SD} and lab measured $C_{Chl\text{-}a}$. The logarithmic function obtained between "Z_{SD} and $C_{Chl\text{-}a}$" (Equation No. 8) was substituted into Equation No. (9) originally proposed by (Carlson, 1977), resulting in Equation No. 10. Equation 10 is a revised version of Carlson's model for evaluation of TSI_{FHL}. The results obtained from TSI (Z_{SD}) were compared with criteria established in the

peer-reviewed literature (Table 4). The evaluation standards for TSI_{FHL}, corresponding to $C_{Chl\text{-}a}$ were categorized into six classes (Table 5).

$$lnZ_{SD} = \propto lnC_{Chl-a} + \beta \quad (8)$$

$$TSI\ (Z_{SD}) = 10\left(6 - \frac{lnZ_{SD}}{ln2}\right) \quad (9)$$

$$TSI\ (C_{Chl-a})_{FHL} = 10\ [6 - \left(\frac{\propto lnC_{Chl-a} + \beta}{ln2}\right)] \quad (10)$$

where, α and β are the angular and linear coefficients respectively. TSI $(C_{Chl\text{-}a})_{FHL}$ is Trophic State Index for freshwater Himalayan lake with respect to concentration of Chl-a. $C_{Chl\text{-}a}$ represents concentration of Chlorophyll-a in µg/L, Z_{SD} represents Secchi disk depth in m.

4. Results and discussion

4.1. Landsat 8 OLI reflectance spectra of lake water (ρw)

Fig. 2 exemplifies the ρw in visible to near infrared region (452 – 851 nm) of surveyed sample points in Wular lake during October 2018. ρw displayed higher variability in the visible and near infra-red regions. The spectral features of Chl-a were relatively highlighted in the reflectance spectrum even for samples with low $C_{Chl\text{-}a}$. The low spectra at ~ < 500 nm, is caused by the absorption of algal pigments as well as dissolved organic matter (Gitelson et al., 1993). The maxima ρw touched 7% in the green region (which varies from 0.056 - 0.076 with average of 0.068), is due to the relatively lower absorption of green light by algae and because of increased backscattering with increase in particle concentration (Duan et al., 2007; Gitelson, 1992). A declining tendency of the ρw in red (~ 6%) and NIR (~ 5%) region corresponds to maxima absorption by phytoplankton pigments (Gitelson & Kondratyev, 1991). An increase in ρw beyond 655 nm wavelength corresponds to the fluorescence produced by Chl-a pigments (Gordon, 1979). In productive waters this peak shifts maximum reflectance to longer wavelengths with increase in Chl-a (Gitelson et al., 1993).

$C_{Chl\text{-}a}$ ranged between 6.66 and 29.30 µg/L (mean value of 14.62 µg/L). Z_{SD} varied from 0.20 to 1.08 m with average of 0.51 m (Table 1). The maxima concentration of Chl-a has been witnessed near lake outlet (S_1) in the Southern most part, whereas lowest concentration at S_{18} in the North-western portion of lake, deepest part as per the depth

analysis (1.08 m). The Pearson's Correlation coefficient (PCC) examination between in situ $C_{Chl\text{-}a}$ and Z_{SD} revealed significant negative relationship with r = - 0.87.

4.2. $C_{Chl\text{-}a}$ and Z_{SD} algorithm performance

Table 2 demonstrates the possible outcome of employed regression algorithms in terms of (R^2) for Chl-a and Z_{SD}. Linear form of regression algorithm established more significant correlation between reflectance and Chl-a, while as exponential in case of Z_{SD}. Table 3 depicts the result of best fit regression algorithm for Chl-a and Z_{SD} with values of error approximations. In case of Chl-a, the best linear relationship has been witnessed for [ρw (865) – ρw (482) / ρw (561)] with highest R^2 = 0.89 (Fig. 3 (a)), whereas in case of Z_{SD} non-linear relationship resulted in highest value of R^2=0.84 for [ρw^{-1} (865)] (Fig. 3 (b)). The calibration outcome signifies the acceptable linearity of single band and three-band model for remote estimation of Z_{SD} (Equation. No. 11) and $C_{Chl\text{-}a}$ (Equation. No.12) respectively, expressed by:

$$Z_{SD} = 0.01 \times \exp\left[0.51 \times \left(\rho w^{-1}(865)\right)\right] \qquad (11)$$

$$\text{Cchl} - \text{a} = 126.27 + 62.24 \times \left[\frac{(\rho w\ (865) - \rho w(482)}{\rho w\ (561)}\right] \qquad (12)$$

where, $C_{Chl\text{-}a}$ and Z_{SD} is Chlorophyll-a concentration (in μg/L) and Secchi disk depth (in m) respectively. ρw is the calibrated spectral reflectance after DOS correction. 482, 561, and 865 are Landsat 8 OLI band central wavelengths for blue, green and NIR region respectively.

In present study, Blue–Green–NIR bands show their maximum sensitivity to evaluate the phytoplankton pigments. The visible (Blue to Green) and near infrared (NIR) bands have been generally applied to find out the relationship between biophysical parameters and surface reflectance for lake studies (Sass et al., 2007). Gitelson et al., (2003, 2005) proposed a three-band reflectance model for assessing pigment contents in terrestrial vegetation which was further used to estimate chlorophyll-a concentrations in turbid waters (Dall'Olmo et al., 2003; Gitelson et al., 2007, 2008). Singh et al., (2014) successfully applied (R^2 of 0.88) the three-band model for retrieval of Chlorophyll-a in Hypersaline–Alkaline Water Using Landsat ETM+ Sensor. Watanabe et al., (2015) detected reasonable fits from Landsat-8 OLI bands with R^2 greater than 0.70 for NIR-Green, NIR-Blue and, NIR-Red ratios.

For Z_{SD} ranging from 0.17 - 0.75 m (average of 0.49 m) a reasonable relationship (R^2 = 0.78) has been observed between Landsat 8 OLI single band model (Equation No. 11) and in situ Z_{SD}. In case of $C_{Chl\text{-}a}$ varying from 7.87 - 31.51 μg/L with average of 15.05 μg/L, the

Landsat 8 OLI three-band model (Equation No. 12) exhibited very close relationships (R^2 = 0.99) with lab measured $C_{Chl\text{-}a}$. The difference between measured and modeled $C_{Chl\text{-}a}$ and Z_{SD} for 20 sample points estimated using bias (Fig. 4 a, b) showed bias of -0.43 µg/L and 0.02 µg/L respectively. For $C_{Chl\text{-}a}$ maximum and minimum difference has been observed at S_1 (2.21) and S_{19} (0.02) located in the North-western and middle portion of the lake respectively. For Z_{SD}, maximum difference of 0.34 has been observed at S_{18}, and zero for S_2.

The predicted model has been validated using independent validation subclass i.e. 20% samples to estimate the applicability of the proposed model of $C_{Chl\text{-}a}$ and Z_{SD} (Fig. 5 a, b). The efficiency of linear NIR-Blue-Green model exhibited the acceptable results in validation for Chl-a. The model showed SEE of 0.77 µg/L, MAPE of 5.8% and E of 0.98 µg/L. In case of Z_{SD} the errors associated with the exponential single band (NIR) model, calculated as 0.11 µg/L, 13.93%, and 0.77 µg/L for SEE, MAPE, and E respectively. Yüzügüllü & Aksoy, (2011) studied the relationship between Z_{SD} and reflectance data in Lake Eymir using Quickbird satellite data and observed higher correlation with NIR band and attributed to the higher turbidity level and shallow depth of water. Lee et al., (2016) confirmed the spectral band setting of Landsat 8 OLI is suitable for the assessment of Z_{SD}. The outcomes clearly suggest that the models established for FHL using simulated Landsat 8 OLI bands yielded satisfactory performances.

4.3. Mapping of $C_{Chl\text{-}a}$ and Z_{SD} using Landsat 8 OLI

The method illustrated in Section 3.3 were employed to Landsat 8 OLI image to map $C_{Chl\text{-}a}$ and Z_{SD} at 30 m spatial resolution for the open waters covering North-western and southern fringe of the lake Fig. 6 (a, b). Area covered with highly dense aquatic vegetation particularly with Azolla cristata was not mapped as it hides the true reflectance of the water. The ρw of Landsat 8 OLI seemed valid and reliable with this turbid lake system because the temporal gap between in situ measurements and Landsat 8 acquisition was only 4 days. The values of $C_{Chl\text{-}a}$ in the range of 25.81-115.51 µg/L was apparent in the shallow areas at the periphery of lake generally covered with dense algal bloom. The upper limit of $C_{Chl\text{-}a}$ > 207.96 µg/L was noticeable in the Northern part of the lake. Primarily due to the mixing of water from river Jhelum, Erin, and Madhumati lying near the major townships, enhancing concentration of nutrients in the lake (Mushtaq et al., 2015; Mushtaq & Nee Lala, 2017a). The lowermost concentration of $C_{Chl\text{-}a}$ < 25.81 µg/L is confined in the central part of lake having depth > 0.66 m.

The spatial analysis revealed that most of the pixels (70.51% of the open water lake area) had Chl-a values < 25.81 µg/L, whereas 29.49% area have values on the higher side as per the classification criteria of Carlson, (1977); Carlson & Simpson, (1996) (Table 4). Z_{SD} an important parameter for indication of turbidity level, manifest the turbid nature of lake water. For the time considered, the spatial pattern of Z_{SD} exhibited the maximum and minimum depth of 0.82 m and 0.02 m respectively with average of 0.50 m. In general, the pattern of higher transparency (Z_{SD} > 0.66 m) was seen further offshore whereas lower clarity (Z_{SD} < 0.18 m) is nearby river inlets and peripheral areas. The depth analysis exhibited that 41.1% of the total clear water portion is under depth greater than 0.66 m, while as 16.6% is under 0.18 m. Even though, depth > 0.66 m covers major portion of lake waters, on the contrary 42.28% comes under the depth of 0.18 m - 0.66 m, which points towards the shallowness of waterbody. It was clear that the values of both $C_{Chl\text{-}a}$ and Z_{SD} tend to classify the water for higher trophic levels.

4.4. Landsat 8 OLI derived TSI_{FHL}

The TSI_{FHL}, developed using regression analysis between lab measured and in-situ data of $C_{Chl\text{-}a}$ and Z_{SD} showed a significant correlation in logarithmic fit (Fig. 7) with $R^2 = 0.86$ and $\rho = 0.01$. The final equation (Equation No. 10) was used to define the trophic state of Wular lake at the time of investigation (October 2018) with the incorporation of Landsat 8 OLI derived Chl-a given by the equation No. 13

$$TSI\ (C_{Chl-a})_{FHL} = 10\left[6 - \left(\frac{-0.495\ lnChla + 1.7934}{ln2}\right)\right] \qquad (13)$$

The TSI_{FHL} for the month of October (Fig. 8 (a)) varied from lower and upper limit of 42.78 to 75.96 with average value of 55.03. The TSI_{FHL} values obtained were classified under six different trophic categories viz oligotrophic, mesotrophic, light eutrophic, medium eutrophic, hypereutrophic, and extremely hypereutrophic (Table 5). The lowest value of TSI_{FHL} witnessed in the middle portion of lake with depth greater than 0.66 m comes under the mesotrophic level. The mesotrophic level covers 42.97 % of the total lake area (open water). However, as the depth decreases towards the marginal areas, the trophic level starts to rise to eutrophic state (light eutrophic to hypereutrophic), which covers 51.02 % of total open water portion of ~ 18 km^2. The light eutrophic class covers 3.99 km^2 (22.34 %), medium eutrophic covers 2.84 km^2 (15.93 %) while as hypereutrophic and extremely hypereutrophic covers

12.74 % and 6.02 % respectively. At the convergence point of rivers (Erin, Madhumati and Jhelum) in North nearest to major urban settlements (Bandipora district), it exhibits hypereutrophic state. Although, the spatial analysis revealed that most of the pixels (42.97 %) had TSI_{FHL} values in the mesotrophic range, however the results evidently specify that 57.03 % of lake area has been found under light eutrophic state to extremely hypereutrophic state during the time of investigation (Table 4).

Furthermore, the trophic classification of Wular lake based on Z_{SD} (Fig. 8 (b)) tends to classify the water for very higher trophic category as per the classification criteria given in Table 4 (Aizaki et al., 1981; Carlson, 1977; Carlson & Simpson, 1996; Vollenweider & Kerekes, 1982). The trophic state classification based on Z_{SD} as per the Equation no. 9 leads to the overestimation of values which do not correlate with values obtained from TSI_{FHL}. TSI (Z_{SD}) classified the deepest water of the lake (mesotrophic class as per TSI_{FHL}) under eutrophic category (53.23%). According to (Carlson, 1980; Mannino et al., 2008) care should be taken while classifying inland waters using Secchi disk as transparency exhibit the combined effect of algal as well as inorganic particles. Watanabe et al., (2015) detected classification of trophic state of Barra Bonita Hydroelectric Reservoir in Brazil by Secchi disk opposite to chlorophyll-a.

The foremost causative factor behind the higher trophic level is due to the radical change in LULC, particularly cultivated lands, decreased forest cover, unplanned urbanization which contribute high nutrient loads (Liu et al., 2010; Mushtaq & Lala, 2017; Wang et al., 2011, 2013; Wu & Wang 2012). A drastic transformation in the form of unplanned urban sprawl comprising of built-up areas (increased from 7 km^2 to 52 km^2 during 1992 - 2008), which exists in the vicinity of lake contributes huge amount of nutrient load to lake from major rivers and other small tributaries due to the improper drainage system (Mushtaq & Pandey, 2013). Another major factor is the degradation of forest land and increased soil erosion (Mushtaq et al., 2018), which augments the nutrient discharge which comprises the major source of particulate Phosphorus (Panagopoulos et al., 2011). Hence, the direct and indirect dumping of wastes from various human related activities roots to heavy deposition of chemicals and nutrients causing the lake water highly polluted, and subsequent eutrophication. Besides there is a massive reduction in clear water dominated area of lake (from 77 km^2 to 6 km^2) and upsurge in lake surface water temperature (Mushtaq & Nee Lala, 2017b; Mushtaq et al., 2019), resulting in dominance of algal laden waters. Butt & Nazeer, (2015) revealed the key aspect behind the increased quanity of Chl-a and higher TSI in Rawla lake, Pakistan due to the relatively moderate temperature in the month of October

(average 20º C), feasible for algal growth. The study pertaining to the interrelationship of water quality and lake surface water temperature on the Dianchi Lake, noticed the lake surface tempearture as foremost factor behind the development of algal bloom (Yang et al., 2018). Tang et al., (2019) stated that the alterations in the lake's trophic state leads to the change in structure of plankton community and species composition. It has already been investigated and documented by Keller et al., (2018) that there is already elevated proliferation and predominance of invasive species of Azolla cristata and Alternanthera philoxerodies (alligator weed), which forms the thick algal mats. If the current conditions of polluting the lake is sustained, it is projected that the lake will lead to further deterioration in near future.

5. Conclusion

Remote estimation of $C_{Chl\text{-}a}$ and Z_{SD} using Landsat 8 OLI data is very effective and reliable technique in case of large and inaccessible water body. The overarching aim of the present work has been the scrutinizing the trophic status of the lake with Landsat 8 OLI data by means of new form of TSI derived from remotely estimated $C_{Chl\text{-}a}$ and Z_{SD} for freshwater lake in Kashmir Himalayas. The remotely sensed average $C_{Chl\text{-}a}$ concentration for the Wular lake was 28.7 µg/L with mean Z_{SD} of 0.50 m. The depth analysis revealed that 42.28 % of the lake area is falling under the depth range of 0.18 m - 0.66 m, clearly indicating the highly turbid conditions. The results of R^2 and error metrics showed the performance and robustness of predicted model for $C_{Chl\text{-}a}$ ($R^2 = 0.89$) and Z_{SD} ($R^2 = 0.84$). Further, the results highlighted the justification behind the theoretical model with an acceptable degree of certainty ($R^2 = 0.96$) and established the robustness of Chl-a model as an effective tool for retrieval of TSI in turbid water of Himalayan lake. The spatial analysis of TSI_{FHL} for Wular lake (in the range of 42.78 to 75.96) showed that 57.03 % of lake area in the open waters fall under the light eutrophic to extremely hyper-eutrophic state for the period considered. This is apparent as unplanned urbanization and extensive transformations in land systems are contaminating the lake waters, directly or indirectly. This condition is not only distressing for locals who are dependent on lake water for drinking purpose and livelihood, but also for migratory waterbirds, fish resources, and the local environment. The TSI_{FHL} index proposed in this study was found more suitable for Himalayan lake ecosystems. However, the use of TSI_{FHL} in other waterbodies with long term data is encouraged to further validate its aptness. The present study emphasizes the urgent need of eutrophication management and controlling

nutrient inputs for retaining the clear water state as augmented profusion of algal blooms can evidently deteriorate and reduce ecosystem services of Wular lake in future.

Acknowledgment

First, the authors would like to express thanks to NASA for making the Landsat data sets freely available in the University of Maryland under the umbrella of GLCF and USGS web server. The authors are thankful to Centre of Research for Development (CORD), University of Kashmir, and Office of the Assistant Executive Engineer PHE, Chemical/Water Quality Sub Division, Srinagar, J&K for providing the laboratory facilities.

Data Avaliablity Statement

The cloud-free Landsat 8 OLI Level 1T image used in this research can be downloaded from USGS Earth Explorer data portal https://earthexplorer.usgs.gov/.

Funding

The authors acknowledge the financial aid provided by the Science and Engineering Research Board, a statutory body of the Department of Science & Technology, Government of India to carry out current research work

Disclosure statement

No potential conflict of interest was reported by the authors.

References

Aizaki, M., Otsuki, A., Fukushima, T., Hosomi, M., Muraoka, K. (1981). Application of Carlson's trophic state index to Japanese lakes and relationships between the index and other parameters. Internationale Vereinigung für theoretische und angewandte Limnologie: Verhandlungen, 21, 675-681. https://doi.org/10.1080/03680770.1980.11897067

Bohn, V.Y., Carmona, F., Rivas, R., Lagomarsino, L., Diovisalvi, N., Zagarese, H.E. (2018). Development of an empirical model for chlorophyll-a and Secchi Disk Depth estimation for a Pampean shallow lake (Argentina). The Egyptian Journal of Remote Sensing and Space Sciences, 21, 183-191. https://doi.org/10.1016/j.ejrs.2017.04.005

Bresciani, M., Cazzaniga, I., Austoni, M., Sforzi, T., Buzzi, F., Morabito, G., Giardino, C. (2018). Mapping phytoplankton blooms in deep subalpine lakes from Sentinel-2A and Landsat-8. Hydrobiologia, 824, 197–214. https://doi.org/10.1007/s10750-017-3462-2

Bukata, R. P. (2013). Retrospection and introspection on remote sensing of inland water quality: "Like Déjà Vu All Over Again." Journal of Great Lakes Research, 39, 2-5. https://doi.org/10.1016/j.jglr.2013.04.001

Butt, M.J., Nazeer, M. (2015). Landsat ETM+ Secchi Disc Transparency (SDT) Retrievals for Rawal Lake, Pakistan. Advances in Space Research, https://doi.org/10.1016/j.asr.2015.06.041

Carlson R.E. (1977). A trophic state index for lakes. Limnology and Oceanography, 22, 361-369. https://doi.org/10.4319/lo.1977.22.22.0361

Carlson, R.E. (1980). More complications in the chlorophyll-Secchi disk relationship. Limnology and Oceanography, 25, 379–382. https://doi.org/10.4319/lo.1980.25.2.0379

Carlson, R.E., Simpson, J. (1996). A Coordinator's Guide to Volunteer Lake Monitoring Methods. North American Lake Management Society. 96pp.

Chávez, P. S. J. (1996). Image-based atmospheric corrections - revisited and improved. Photogrammetric Engineering and Remote Sensing, 62, 1025–1036. https://doi.org/0099-1112/96/6209-1025

Chen, Jiang, Zhu, W., Tian, Y. Q., Yu, Q., Zheng, Y., Huang, L. (2017). Remote estimation of colored dissolved organic matter and chlorophyll-a in Lake Huron using Sentinel-2 measurements. Journal of Applied Remote Sensing, 11(03), 1. https://doi.org/10.1117/1.jrs.11.036007

Chen, Jun, Wen, Z., Xiao, Z. (2011). Spectral Geometric Triangle Properties of Chlorophyll-A Inversion in Taihu Lake Based on TM Data. Journal of Water Resource and Projection, 3, 67-75. https://doi.org/10.4236/jwarp.2011.31008

Chen, Jun, Zhang, M., Cui, T., Wen, Z. (2013). A review of some important technical problems in respect of satellite remote sensing of chlorophyll - A concentration in coastal waters. IEEE Journal of Selected Topics in Applied Earth Observations and Remote Sensing, 6, 2275–2289. https://doi.org/10.1109/JSTARS.2013.2242845

Cunha, D. G. F., Calijuri, M. do C., Lamparelli, M. C. (2013). A trophic state index for tropical/subtropical reservoirs (TSItsr). Ecological Engineering, 60, 126–134. https://doi.org/10.1016/j.ecoleng.2013.07.058

Dall'Olmo, G., Gitelson, A. A., Rundquist, D. C. (2003). Towards a unified approach for remote estimation of chlorophyll-a in both terrestrial vegetation and turbid productive waters. Geophysical Research Letters, 30, 1038. https://doi.org/10.1029/2003GL018065

Dekker, A.G., Peters, S.W.M. (1993). The use of the Thematic Mapper for the analysis of eutrophic lakes: A case study in the Netherlands. International Journal of Remote Sensing, 14, 799-821. https://doi.org/10.1080/01431169308904379

Dickey, T., Lewis, M., Chang, G. (2006). Optical oceanography: Recent advances and future directions using global remote sensing and in situ observations. Reviews of Geophysics, 44. https://doi.org/10.1029/2003RG000148

Dua, H., Chen, Z., Mao, G., Chen, L., Crittenden, J., Li, R.Y.M., Chai, L. (2019). Evaluation of eutrophication in freshwater lakes: A new non-equilibrium statistical approach. Ecological Indicators, 102, 686–692. https://doi.org/10.1016/j.ecolind.2019.03.032

Duan, H., Zhang, Y., Zhang, B., Song, K., Wang, Z. (2007). Assessment of chlorophyll-a concentration and trophic state for lake chagan using landsat TM and field spectral data. Environmental Monitoring and Assessment, 129, 295–308. https://doi.org/10.1007/s10661-006-9362-y

French, T. D., Petticrew, E. L. (2007). Chlorophyll a seasonality in four shallow eutrophic lakes (northern British Columbia, Canada) and the critical roles of internal phosphorus loading and temperature. Hydrobiologia, 575, 285–299. https://doi.org/10.1007/s10750-006-0377-8

Giardino, C., Pepe, M., Brivio, P. A., Ghezzi, P., Zilioli, E. (2001). Detecting chlorophyll, Secchi disk depth and surface temperature in a sub-alpine lake using Landsat imagery. Science of the Total Environment, 268, 19–29. https://doi.org/10.1016/S0048-9697(00)00692-6

Gitelson, A. A. (1992). The peak near 700 nm on reflectance spectra of algae and water relationships of its magnitude and position with chlorophyll concentration. International Journal of Remote Sensing, 13, 3367-3373. https://doi.org/10.1080/01431169208904125

Gitelson, A. A., Kondratyev, K. Y. (1991). Optical models of mesotrophic and eutrophic water bodies. International Journal of Remote Sensing, 12, 373-385. https://doi.org/10.1080/01431169108929659

Gitelson, A., Garbuzov, G., Szilagyi, F., Mittenzwey, K. H., Karnieli, A., Kaiser, A. (1993). Quantitative remote sensing methods for real-time monitoring of inland waters quality. International Journal of Remote Sensing, 14, 1269–1295. https://doi.org/10.1080/01431169308953956

Gitelson, Anatoly A., Dall'Olmo, G., Moses, W., Rundquist, D. C., Barrow, T., Fisher, T. R., Gurlin, D., Holz J. (2008). A simple semi-analytical model for remote estimation of chlorophyll-a in turbid waters: Validation. Remote Sensing of Environment, 112, 3582-3593. https://doi.org/10.1016/j.rse.2008.04.015

Gitelson, Anatoly A., Gritz, Y., Merzlyak, M. N. (2003). Relationships between leaf chlorophyll content and spectral reflectance and algorithms for non-destructive chlorophyll assessment in higher plant leaves. Journal of Plant Physiology, 160, 271-282. https://doi.org/10.1078/0176-1617-00887

Gitelson, Anatoly A., Schalles, J. F., Hladik, C. M. (2007). Remote chlorophyll-a retrieval in turbid, productive estuaries: Chesapeake Bay case study. Remote Sensing of Environment, 109, 464–472. https://doi.org/10.1016/j.rse.2007.01.016

Gitelson, Anatoly A., Viña, A., Ciganda, V., Rundquist, D. C., Arkebauer, T. J. (2005). Remote estimation of canopy chlorophyll content in crops. Geophysical Research Letters, 32, L08403. https://doi.org/10.1029/2005GL022688

Glibert, P. M., Landsberg, J. H., Evans, J. J., Al-Sarawi, M. A., Faraj, M., Al-Jarallah, M. A., Haywood, A., Ibrahem, S., Klesius, P., Powell, C., Shoemaker, C. (2002). A fish kill of massive proportion in Kuwait Bay, Arabian Gulf, 2001: The roles of bacterial disease, harmful algae, and eutrophication. Harmful Algae, 1, 215–231. https://doi.org/10.1016/S1568-9883(02)00013-6

Gordon, H. R. (1979). Diffuse reflectance of the ocean: the theory of its augmentation by chlorophyll a fluorescence at 685 nm. Applied Optics, 18, 1161-1166. https://doi.org/10.1364/ao.18.001161

Guo, Y., Li, Y., Zhu, L., Wang, Q., Lv, H., Huang, C., Li, Y. (2016). An Inversion-Based Fusion Method for Inland Water Remote Monitoring. IEEE Journal of Selected Topics in Applied Earth Observations and Remote Sensing, 9, 5599-5611. https://doi.org/10.1109/JSTARS.2016.2615125

Gurlin, D., Gitelson, A. A., Moses, W. J. (2011). Remote estimation of chl-a concentration in turbid productive waters - Return to a simple two-band NIR-red model. Remote Sensing of Environment, 115, 3479–3490. https://doi.org/10.1016/j.rse.2011.08.011

Ha, N. T. T., Thao, N. T. P., Koike, K., Nhuan, M. T. (2017). Selecting the best band ratio to estimate chlorophyll-a concentration in a tropical freshwater lake using sentinel 2 A imagesfrom a case study of Lake Ba Be (Northern Vietnam). ISPRS International Journal of Geo-Information, 6(9). https://doi.org/10.3390/ijgi6090290

Han, X., Feng, L., Chen, X., Yesou, H. (2014). MERIS observations of chlorophyll-a dynamics in Erhai Lake between 2003 and 2009. International Journal of Remote Sensing, 35, 8309-8322. https://doi.org/10.1080/01431161.2014.985395

Holm-Hansen, O., Riemann, B. (2006). Chlorophyll a Determination: Improvements in Methodology. Oikos, 30, 438. https://doi.org/10.2307/3543338

Huang, T.L., Li, X., Ma, W.X., Qin, C.H., Zhang, Y.T. (2014). Dynamic characteristics of nutrients and causal analysis in eutrofic reservoir: A case study of Shibianyu reservoir. Desalination and Water Treatment, 52, 1624-1635. https://doi.org/10.1080/19443994.2013.846406

Huot, Y., Babin, M., Bruyant, F., Grob, C., Twardowski, M. S., Claustre, H. (2007). Relationship between photosynthetic parameters and different proxies of phytoplankton biomass in the subtropical ocean. Biogeosciences, 4, 853–868. https://doi.org/10.5194/bg-4-853-2007

Jeelani, G., Feddema, J.J., Veen, C.J.V.D., Stearns, L. (2012). Role of snow and glacier melt in controlling river hydrology in Liddar watershed (western Himalaya) under current and future climate. Water Resources Research, 48,W12508. https://doi.org/10.1029/2011WR011590

Kasprzak, P., Padisák, J., Koschel, R., Krienitz, L., Gervais, F. (2008). Chlorophyll a concentration across a trophic gradient of lakes: An estimator of phytoplankton biomass? Limnologica, 38, 327-338. https://doi.org/10.1016/j.limno.2008.07.002

Keller, R. P., Masoodi, A., Shackleton, R. T. (2018). The impact of invasive aquatic plants on ecosystem services and human well-being in Wular Lake, India. Regional Environmental Change. https://doi.org/10.1007/s10113-017-1232-3

Le, C., Hu, C., English, D., Cannizzaro, J., Kovach, C. (2013). Climate-driven chlorophyll-a changes in a turbid estuary: Observations from satellites and implications for management. Remote Sensing of Environment, 130, 11-24. https://doi.org/10.1016/j.rse.2012.11.011

Lee, Z., Shang, S., Qi, L., Yan, J., Lin, G. (2016). A semi-analytical scheme to estimate Secchi-disk depth from Landsat-8 measurements. Remote Sensing of Environment, 177, 101–106. https://doi.org/10.1016/j.rse.2016.02.033

Li, X., Sha, J., Wang, Z. L. (2017). Chlorophyll-A Prediction of lakes with different water quality patterns in China based on hybrid neural networks. Water (Switzerland), 9(7). https://doi.org/10.3390/w9070524

Li, Ying, Cao, W., Su, C., Hong, H. (2011). Nutrient sources and composition of recent algal blooms and eutrophication in the northern Jiulong River, Southeast China. Marine Pollution Bulletin, 63, 249–254. https://doi.org/10.1016/j.marpolbul.2011.02.021

Lillesand, T., Kiefer, R.K., Chipman, J. (2015). Remote Sensing and Image Interpretation, 7th ed.;Wiley: Hoboken, NJ,USA, 2015

Lim, J., Choi, M. (2015). Assessment of water quality based on Landsat 8 operational land imager associated with human activities in Korea. Environmental Monitoring and Assessment, 187, 1–17. https://doi.org/10.1007/s10661-015-4616-1

Liu, C., Liu, L., Shen, H. (2010). Seasonal variations of phytoplankton community structure in relation to physico-chemical factors in Lake Baiyangdian. China. Procedia Environmental Science, 1622–1631. https://doi.org/10.1016/j.proenv.2010.10.173

Lorenzen, C. J. (1967). Determination of Chlorophyll and Pheo-Pigments: Spectrophotometric Equations. Limnology and Oceanography, 12, 343–346. https://doi.org/10.4319/lo.1967.12.2.0343

Lu, D., Mausel, P., Brondizio, E., Moran, E. (2002). Assessment of atmospheric correction methods for landsat tm data applicable to amazon basin lba research. International Journal of Remote Sensing, 23, 2651–2671. https://doi.org/10.1080/01431160110109642

Ma, R., Dai, J. (2005). Investigation of chlorophyll-a and total suspended matter concentrations using landsat ETM and field spectral measurement in Taihu Lake, China. International Journal of Remote Sensing, 26, 2779–2795. https://doi.org/10.1080/01431160512331326648

Mannino, A., Russ, M. E., Hooker, S. B. (2008). Algorithm development and validation for satellite-derived distributions of DOC and CDOM in the U.S. Middle Atlantic Bight. Journal 657 of Geophysical Research: Oceans, 13. https://doi.org/10.1029/2007JC004493

Matus-Hernandez, M. A., Hernandez-Saavedra, N.Y., Martınez-Rincon, R.O. (2018). Predictive performance of regression models to estimate Chlorophyll-a concentration based on Landsat imagery. PLoS ONE, 13(10): e0205682. https://doi.org/10.1371/journal.pone.0205682

Mayo, M., Gitelson, A., Yacobi, Y. Z., Ben-Avraham, Z. (1995). Chlorophyll distribution in Lake Kinneret determined from Landsat Thematic Mapper data. International Journal of Remote Sensing, 16, 175–182. https://doi.org/10.1080/01431169508954386

McFeeters, S.K. (1996). The use of normalized difference water index (NDWI) in the delineation of open water features. International Journal of Remote Sensing,17, 1425-1432. https://doi.org/10.1080/01431169608948714

Moses, W. J., Gitelson, A. A., Berdnikov, S., Povazhnyy, V. (2009). Satellite estimation of chlorophyll-a concentration using the red and NIR bands of MERISThe azov sea case study. IEEE Geoscience and Remote Sensing Letters, 6, 845–849. https://doi.org/10.1109/LGRS.2009.2026657

Murugan, P., Sivakumar, R., Pandiyan, R. (2014). Chlorophyll-A estimation in case-ii water bodies using satellite hyperspectral data. ISRS Proceeding Papers of Sort Interactive Session ISPRS TC VIII International Symposium on Operational Remote Sensing Applications: Opportunities, Progress and Challenges, Hyderabad, India, December 9-12.

Mushtaq, F., Ahmed, P., Ghosh Nee Lala, M. (2019). Spatio-temporal change of surface temperature of Himalayan Lake and its inter-relation with water quality and growth in aquatic vegetation. Geocarto International, 0, 1–17. https://doi.org/10.1080/10106049.2019.1590467

Mushtaq, F., Ahmed, P., Ghosh Nee Lala, M. (2020). Variability of lake surface water temperature: a case study during El Nino and La Nina events over the Himalayan lake region. Physical Geography. https://doi.org/10.1080/02723646.2020.1751386

Mushtaq, F., Lala, M.G.N. (2017). Assessment of hydrological response as a function of LULC change and climatic variability in the catchment of the Wular Lake, J&K, using geospatial technique. Environmental Earth Sciences, 76(22). https://doi.org/10.1007/s12665-017-7065-z

Mushtaq, F., Lala, M.G.N., Wadood, A. (2018). Estimation of soil erosion risk in upper catchment of Wular Lake, Jammu & Kashmir using RUSLE model. International journal of advance research in science and engineering, 7, 1828-1839.

Mushtaq, F., Nee Lala, M.G. (2017a). Remote estimation of water quality parameters of Himalayan lake (Kashmir) using Landsat 8 OLI imagery. Geocarto International, 32, 274–285. https://doi.org/10.1080/10106049.2016.1140818

Mushtaq, F., Nee Lala, M.G. (2017b). Assessment of climatic variability in the catchments of Himalayan Lake, Jammu & Kashmir. Geocarto International, 32, 1090–1104. https://doi.org/10.1080/10106049.2016.1188169

Mushtaq, F., Nee Lala, M.G., Pandey, A.C. (2015). Assessment of pollution level in a Himalayan Lake, Kashmir, using geomatics approach. International Journal of Environmental Analytical Chemistry, 95(11). https://doi.org/10.1080/03067319.2015.1077517

Mushtaq, F., Pandey, A.C. (2013). Assessment of land use/land cover dynamics vis-à-vis hydrometeorological variability in Wular Lake environs Kashmir Valley, India using multitemporal satellite data. Arabian Journal of Geoscience, 7, 4707–4715. https://doi.org/10.1007/s12517-013-1092-1

National Wetland Atlas. (2010). National Wetland Atlas: Jammu and Kashmir, SAC/RESA/AFEG/NWIA/ATLAS/16/2010,18(SAC/EPSA/ABHG/NWIA/ATLAS/34/2011) 18, 120–124.

Paerl, H. W., Paul, V. J. (2012). Climate change: Links to global expansion of harmful cyanobacteria. Water Research, 46, 1349–1363. https://doi.org/10.1016/j.watres.2011.08.002

Palmer, S. C. J., Odermatt, D., Hunter, P. D., Brockmann, C., Présing, M., Balzter, H., Tóth, V. R. (2015). Satellite remote sensing of phytoplankton phenology in Lake Balaton using 10years of MERIS observations. Remote Sensing of Environment, 158, 441-452. https://doi.org/10.1016/j.rse.2014.11.021

Panagopoulos, Y., Makropoulos, C., Mimikou, M. (2011). Diffuse surface water pollution: driving factors for different Geoclimatic regions. Water Resource Management, 25, 3635-3660. https://d oi.org/10.1007/s11269-011-9874-2

Patra, P. P., Dubey, S. K., Trivedi, R. K., Sahu, S. K., Rout, S. K. (2017). Estimation of chlorophyll-a concentration and trophic states in Nalban Lake of East Kolkata Wetland, India from Landsat 8 OLI data. Spatial Information Research, 25, 75–87. https://doi.org/10.1007/s41324-016-0069-z

Ritchie, J. C., Zimba, P. V, Everitt, J. H. (2003). Remote Sensing Techniques to Assess Water Quality. Photogrammetric Engineering and Remote Sensing, 69, 695–704. https://doi.org/10.14358/PERS.69.6.695

Rundquist, D.C., Schalles, J., Peake, J.S. (1995). The response of volume reflectance to manipulated algal concentrations above bright and dark bottoms at various depths in an experimental pool. Geocarto International, 10, 5-14. https://doi.org/10.1080/10106049509354508

Salem, S.I., Higa. H., Kim, H., Kobayashi, H., Oki, K., Oki, T. (2017). Assessment of Chlorophyll-a algorithms considering different trophic statuses and optimal bands. Sensors, 17, 1746. https://doi.org/10.3390/s17081746

Sass, G. Z., Creed, I. F., Bayley, S. E., Devito, K. J. (2007). Understanding variation in trophic status of lakes on the Boreal Plain: A 20 year retrospective using Landsat TM imagery. Remote Sensing of Environment, 109, 127–141. https://doi.org/10.1016/j.rse.2006.12.010

Schalles, J. F. (2006). Optical remote sensing techniques to estimate phytoplankton chlorophyll a concentrations in coastal waters with varying suspended matter and cdom concentrations. In Remote Sensing and Digital Image Processing, 9, 27-79. https://doi.org/10.1007/1-4020-3968-9_3

Senay, G., Shafique, N. (2001). The selection of narrow wavebands for optimizing water quality monitoring on the Great Miami River, Ohio using hyperspectral remote sensor data. Journal of Spatial Hydrology, 1, 1-22.

Singh, K., Ghosh, M., Sharma, S. R., Kumar, P. (2014). Blue-Red-NIR Model for Chlorophyll- a Retrieval in Hypersaline-Alkaline Water Using Landsat ETM + Sensor. IEEE Journal of Selected Topics in Applied Earth Observations and Remote Sensing, 7, 3553–3559. https://doi.org/10.1109/JSTARS.2014.2340856

Smith, V. H. (2006). Responses of estuarine and coastal marine phytoplankton to nitrogen and phosphorus enrichment. Limnology and Oceanography, 51, 377-384. https://doi.org/10.4319/lo.2006.51.1_part_2.0377

Talling, J. F., Golterman, H. L., Clymo, R. S., Ohnstad, M. A. M. (1980). Methods for Physical and Chemical Analysis of Fresh Waters. The Journal of Ecology, https://doi.org/10.2307/2259281

Tang, C., Yia, Y., Yang, Z., Zhou, Y., Zerizghi, T., Wang, X, Cuic, X., Duanc, P. (2019). Planktonic indicators of trophic states for a shallow lake (Baiyangdian Lake, China). Limnologica, 78, 125712. https://doi.org/10.1016/j.limno.2019.125712

Vadeboncoeur, Y., Jeppesen, E., Vander Zanden, M. J., Schierup, H. H., Christoffersen, K., Lodge, D. M. (2003). From Greenland to green lakes: Cultural eutrophication and the loss of benthic pathways in lakes. Limnology and Oceanography, 48, 1408–1418. https://doi.org/10.4319/lo.2003.48.4.1408

Vollenweider, R.A., Kerekes, J. (1982). Eutrophication of Waters. Monitoring, Assessment and Control. Organization for Economic Co-Operation and Development (OECD). Paris, p. 156.

Wang, L., Liang, T. (2015). Distribution Characteristics of Phosphorus in the Sediments and Overlying Water of Poyang Lake. PLoS ONE, 10, e0125859. https://doi.org/10.1371/journal.pone.0125859

Wang, X., Wang, Y., Liu, L., Shu, J., Zhu, Y., Zhou, J. (2013). Phytoplankton and eutrophication degree assessment of Baiyangdian lake wetland, China. The Scientific World Journal, 1–8. https://doi.org/10.1155/2013/436965

Wang, Y., Liu, L., Shu, J., Liu, C., Zhu, Y., Tian, Z. (2011). Community structure of phytoplankton and the water quality assessment in Lake Baiyangdian. Journal of Lake Sciences, 23, 575–58. https://doi.org/10.18307/2011.0413

Watanabe, F. S. Y., Alcântara, E., Rodrigues, T. W. P., Imai, N. N., Barbosa, C. C. F., Rotta, L. H. da S. (2015). Estimation of chlorophyll-a concentration and the trophic state of the barra bonita hydroelectric reservoir using OLI/landsat-8 images. International Journal of Environmental Research and Public Health, 12, 10391-10417. https://doi.org/10.3390/ijerph120910391

Wen, Z., Song, K., Liu, G., Shang, Y., Fang, C., Du, J., Lyu, L. (2018). Quantifying the trophic status of lakes using total light absorption of optically active components. Environmental Pollution, https://doi.org/10.1016/j.envpol.2018.11.058.

Wetlands International. (2007). The comprehensive management action plan on Wular Lake, Kashmir. Wetlands International-South Asia Final Report, New Delhi, p 221

Williamson, C. E., Saros, J. E., Vincent, W. F., Smol, J. P. (2009). Lakes and reservoirs as sentinels, integrators, and regulators of climate change. Limnology and Oceanography, 54, 2273–2282. https://doi.org/10.4319/lo.2009.54.6_part_2.2273

Wu, F.F., Wang, X. (2012). Eutrophication evaluation based on set pair analysis of baiyangdian lake, North China. Procedia Environmental Science, 13, 1030–1036. https://doi.org/10.1016/j.proenv.2012.01.096

Yang, K., Yu, Z., Luo, Y., Yang, Y., Zhao, L., Zhou, X. (2018). Science of the total environment spatial and temporal variations in the relationship between lake water surface temperatures and water quality – a case study of Dianchi Lake. Science of Total Environment, 624, 859-871. https://doi.org/10.1016/j.scitotenv.2017.12.119.

Yang, W., Matsushita, B., Chen, J., Fukushima, T., Ma, R. (2010). An enhanced three-band index for estimating chlorophyll-a in turbid case-II waters: Case studies of Lake Kasumigaura, Japan, and Lake Dianchi, China. IEEE Geoscience and Remote Sensing Letters, 7, 655-659. https://https://doi.org/10.1109/LGRS.2010.204436

Yang, X., Lo, C. P. (2000). Relative radiometric normalization performance for change detection from multi-date satellite images. Photogrammetric Engineering and Remote Sensing, 66, 967–980.

Yu, Q., Wang, H.Z., Li, Y., Shao, J.C., Liang, X.M, Jeppesen, E., Wang, H.J. (2015). Effects of high nitrogen concentrations on the growth of submersed macrophytes at moderate phosphorus concentrations. Water Research, 83, 385-395. https://doi.org/10.1016/j.watres.2015.06.053

Yüzügüllü, O., Aksoy, A. (2011). Determination of Secchi Disc depths in Lake Eymir using remotely sensed data. Procedia - Social and Behavioral Sciences, 19, 586–592. https://doi.org/10.1016/j.sbspro.2011.05.173

Zheng, G., DiGiacomo, P. M. (2017). Remote sensing of chlorophyll-a in coastal waters based on the light absorption coefficient of phytoplankton. Remote Sensing of Environment, 201, 331–341. https://doi.org/10.1016/j.rse.2017.09.008

List of Figures

Fig. 1 Location of Wular Lake in Jammu & Kashmir, three main inflow rivers and sampling locations in True Colour Composite image (Landsat 8 OLI of October 2018).

Fig. 2 Reflectance spectra (ρw) for Landsat 8 OLI bands (452 - 851nm) of sampling points over Wular lake collected in October 2018.

Fig. 3 Scatter plots demonstrates the calibration of the proposed three band model for (a) $C_{Chl\text{-}a}$ and single band model for (b) Z_{SD} between the lab/in-situ measurements and simulated Landsat 8 OLI-based reflectance values.

Fig. 4 Validation of (a) three-band linear (Blue-Green-NIR) model for $C_{Chl\text{-}a}$ and (b) single band exponential (NIR) model for Z_{SD} for Wular lake with independent set of samples.

Fig. 5 Difference between measured and modeled (a) $C_{Chl\text{-}a}$ and (b) Z_{SD} for validation set of samples 20% (n = 4).

Fig. 6 Maps showing spatial distribution of (a) $C_{Chl\text{-}a}$ and (b) Z_{SD} retrieved from Landsat 8 OLI on (Blue-Green-NIR) model and (NIR) model for October 2018.

Fig. 7 Scatter plot displaying cross-relationship between lab measured $C_{Chl\text{-}a}$ and in-situ Z_{SD} for development of TSI_{FHL}.

Fig. 8 (a) Spatial distribution of Landsat 8 OLI derived TSI_{FHL} computed from equation no. 13 for Wular Lake (b) Map displays the spatial distribution of TSI for Wular lake calculated from (Z_{SD}).

Figure 1.

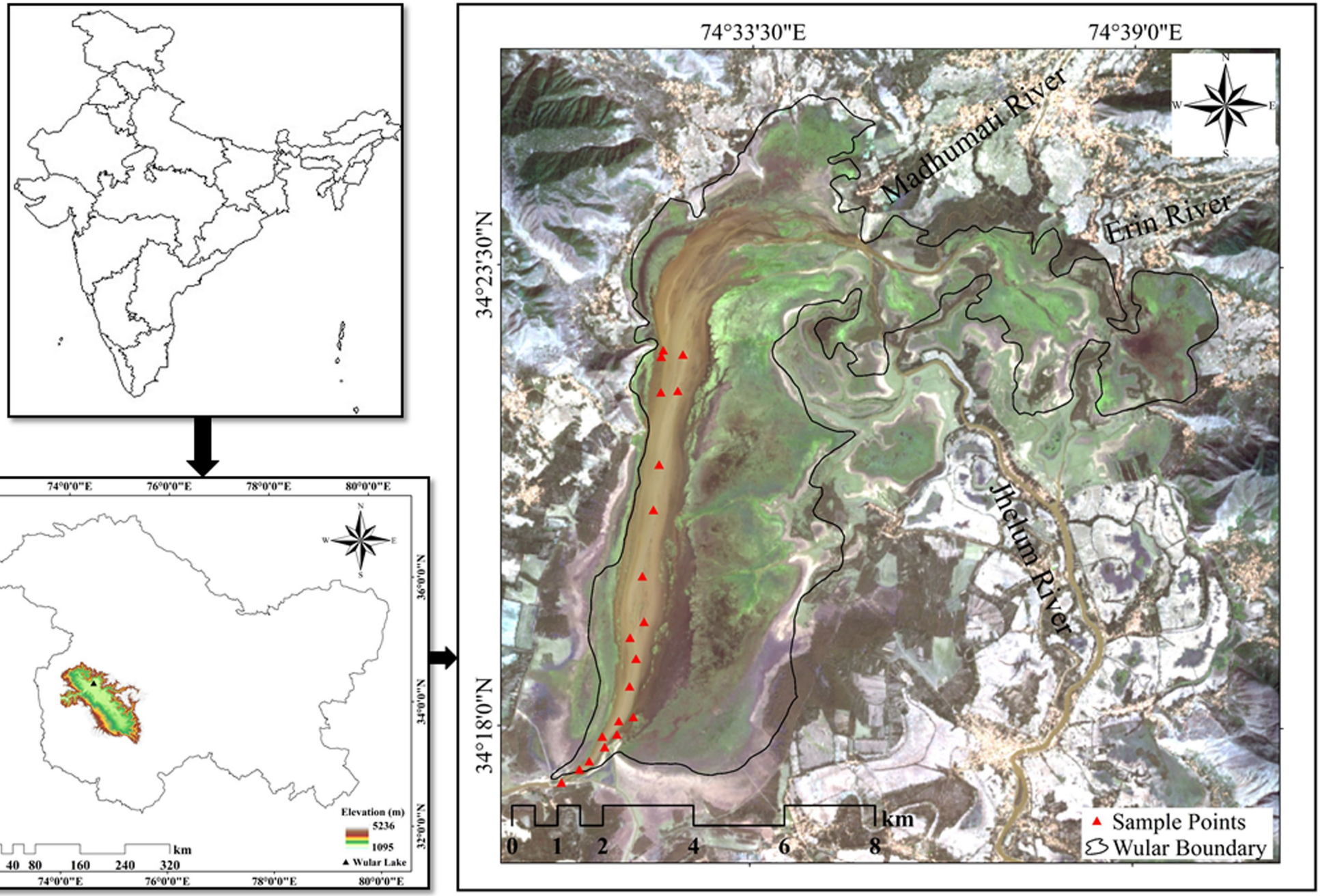
74°33'30"E
74°39'0"E
34°23'30"N
34°18'0"N
Madhumati River
Erin River
Jhelum River
N
S
E
W
0 1 2 4 6 8
km
Sample Points
Wular Boundary
74°0'0"E
76°0'0"E
78°0'0"E
80°0'0"E
36°0'0"N
34°0'0"N
32°0'0"N
0 40 80 160 240 320
km
Elevation (m)
5236
1095
Wular Lake

Figure 2.

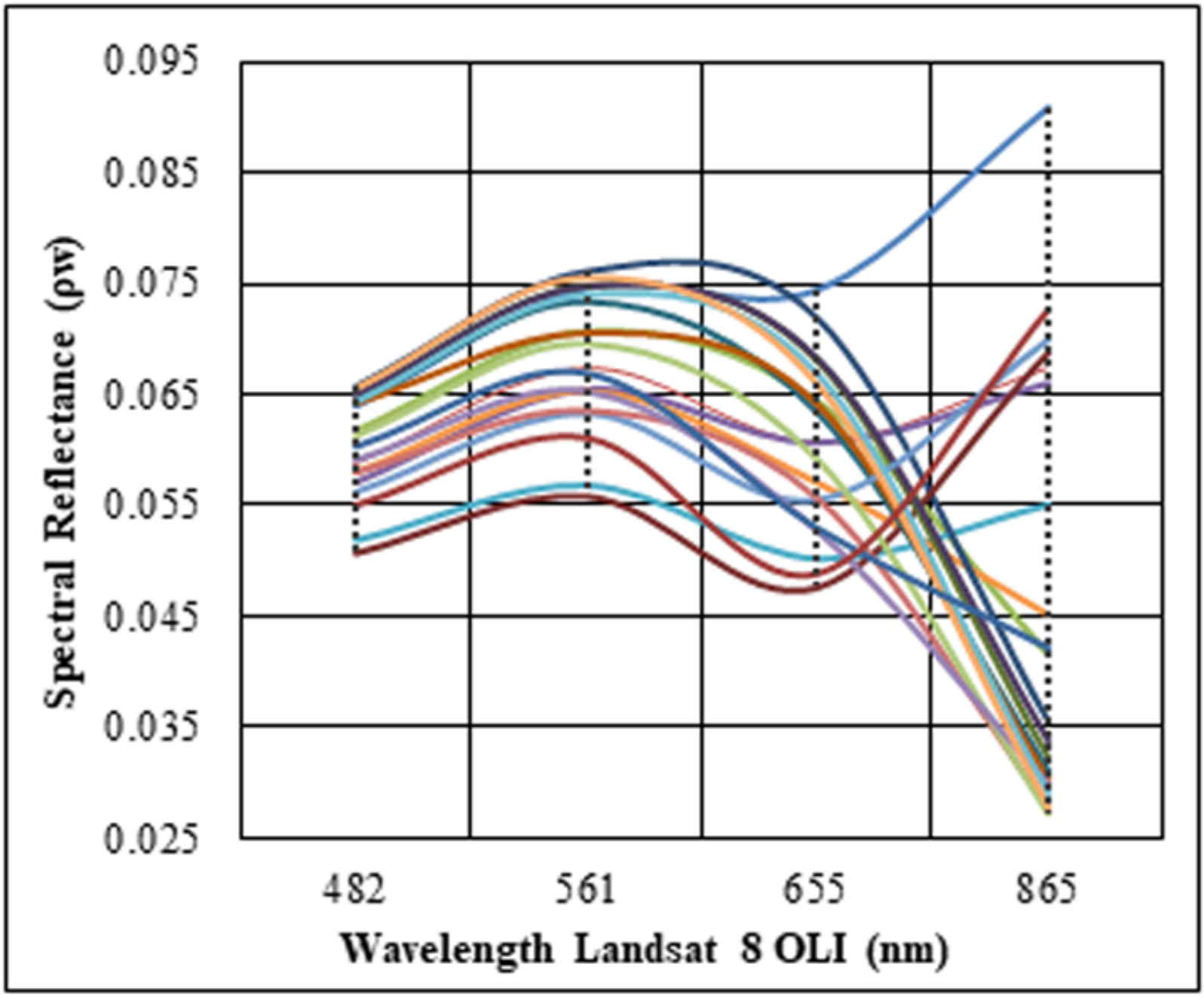
0.095
0.085
0.075
0.065
0.055
0.045
0.035
0.025
Spectral Reflectance (ρw)
482
561
655
865
Wavelength Landsat 8 OLI (nm)

Figure 3.

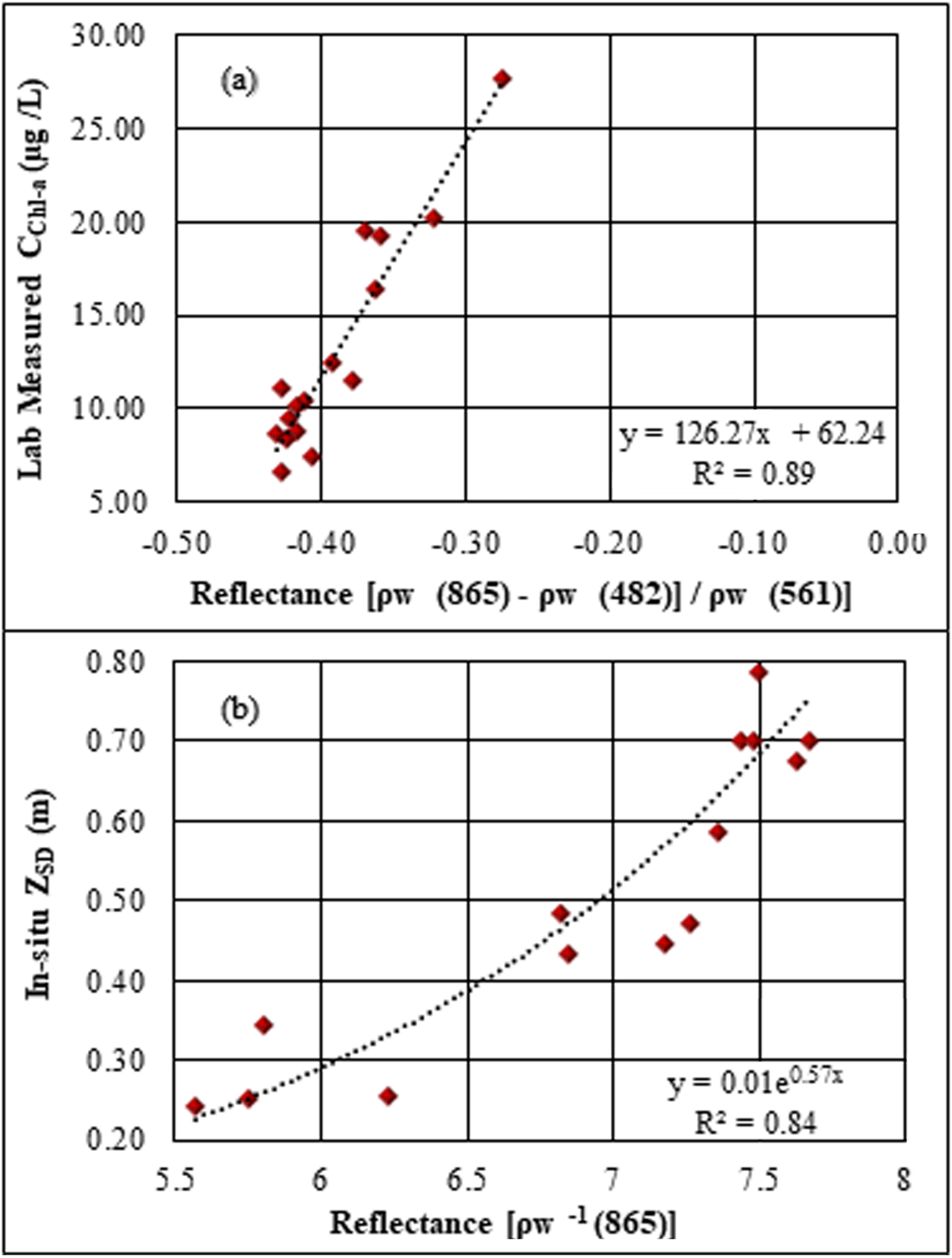
(a)
Lab Measured C_{Chl-a} (µg /L)
30.00
25.00
20.00
15.00
10.00
5.00
-0.50
-0.40
-0.30
-0.20
-0.10
0.00
y = 126.27x + 62.24
R² = 0.89
Reflectance [ρw (865) - ρw (482)] / ρw (561)]
(b)
In-situ Z_{SD} (m)
0.80
0.70
0.60
0.50
0.40
0.30
0.20
5.5
6
6.5
7
7.5
8
y = 0.01e^0.57x
R² = 0.84
Reflectance [ρw -1 (865)]

Figure 4.

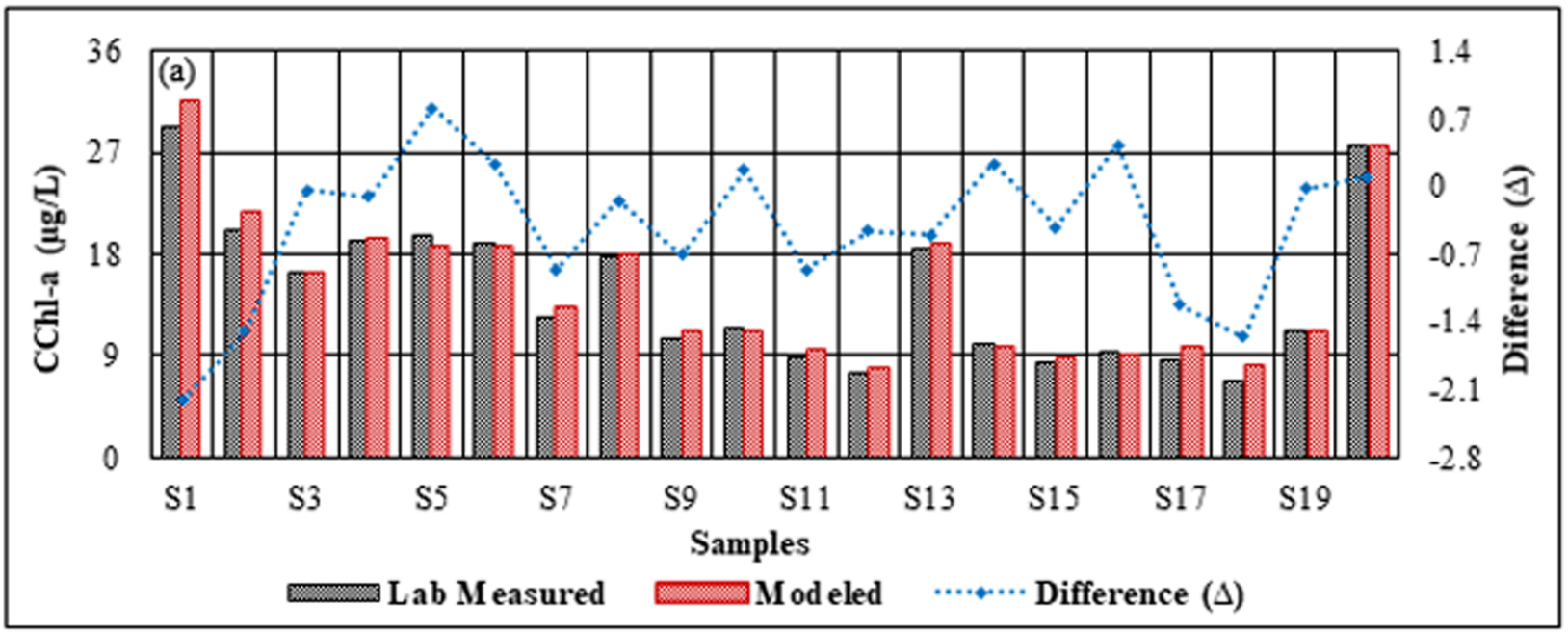
(a)
CChl-a (µg/L)
Difference (Δ)
36
27
18
9
0
1.4
0.7
0
-0.7
-1.4
-2.1
-2.8
S1
S3
S5
S7
S9
S11
S13
S15
S17
S19
Samples
Lab Measured
Modeled
Difference (Δ)

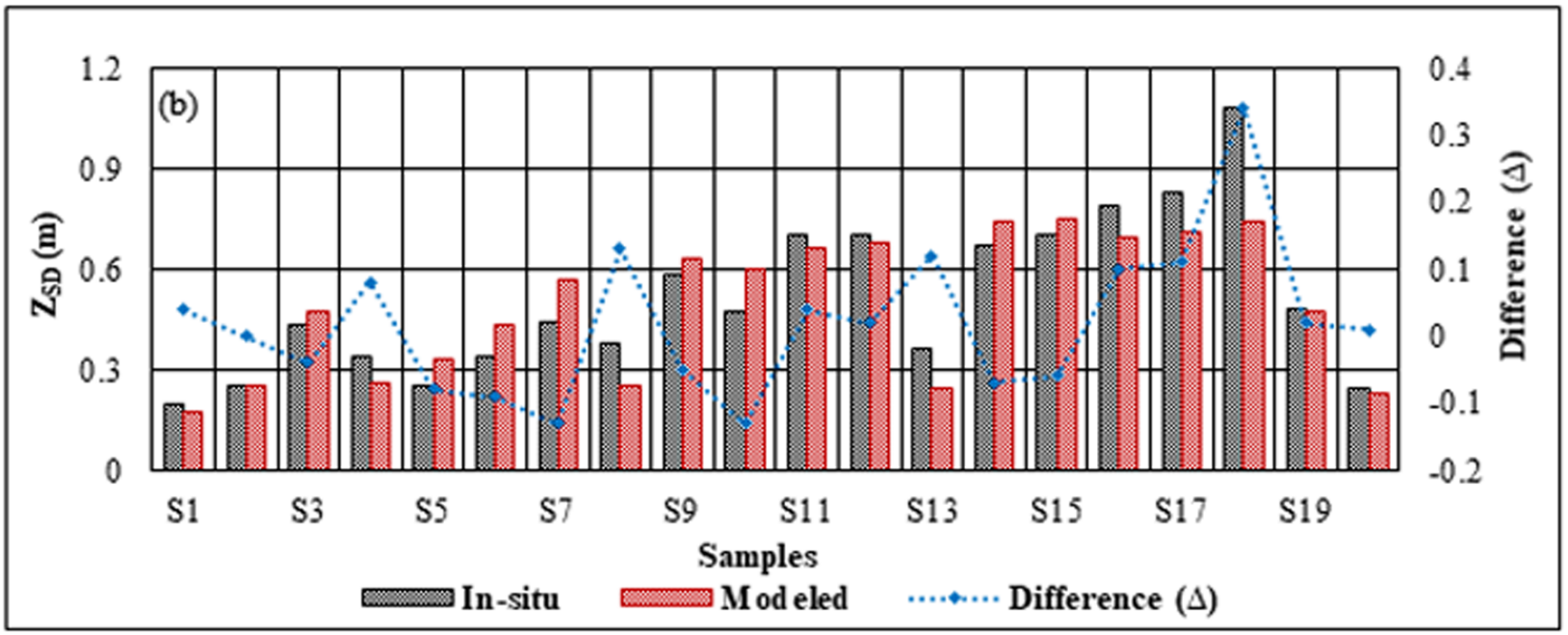
(b)
Z_{SD} (m)
Difference (Δ)
1.2
0.9
0.6
0.3
0
0.4
0.3
0.2
0.1
0
-0.1
-0.2
S1
S3
S5
S7
S9
S11
S13
S15
S17
S19
Samples
In-situ
Modeled
Difference (Δ)

Figure 5.

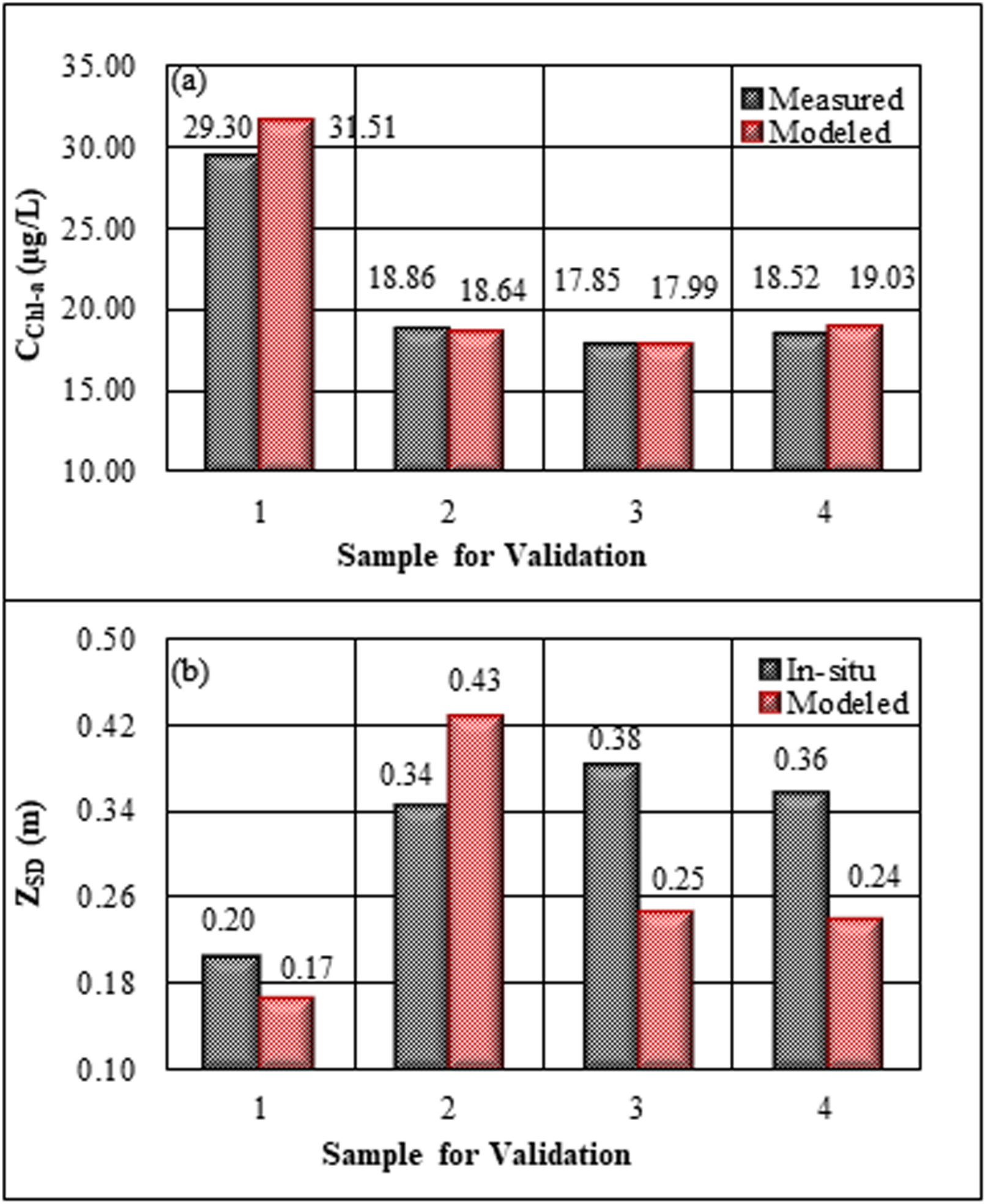
(a)
Measured
Modeled
29.30
31.51
18.86
18.64
17.85
17.99
18.52
19.03
35.00
30.00
25.00
20.00
15.00
10.00
C_{Chl-a} (µg/L)
1
2
3
4
Sample for Validation
(b)
In-situ
Modeled
0.20
0.17
0.34
0.43
0.38
0.25
0.36
0.24
0.50
0.42
0.34
0.26
0.18
0.10
Z_{SD} (m)
1
2
3
4
Sample for Validation

Figure 6.

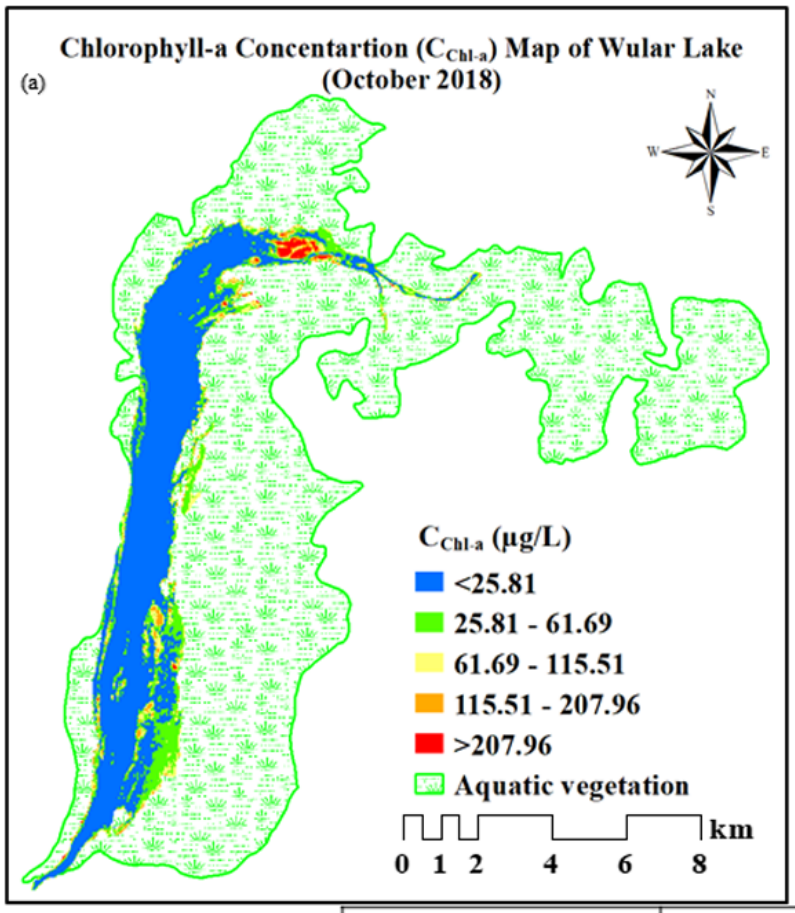

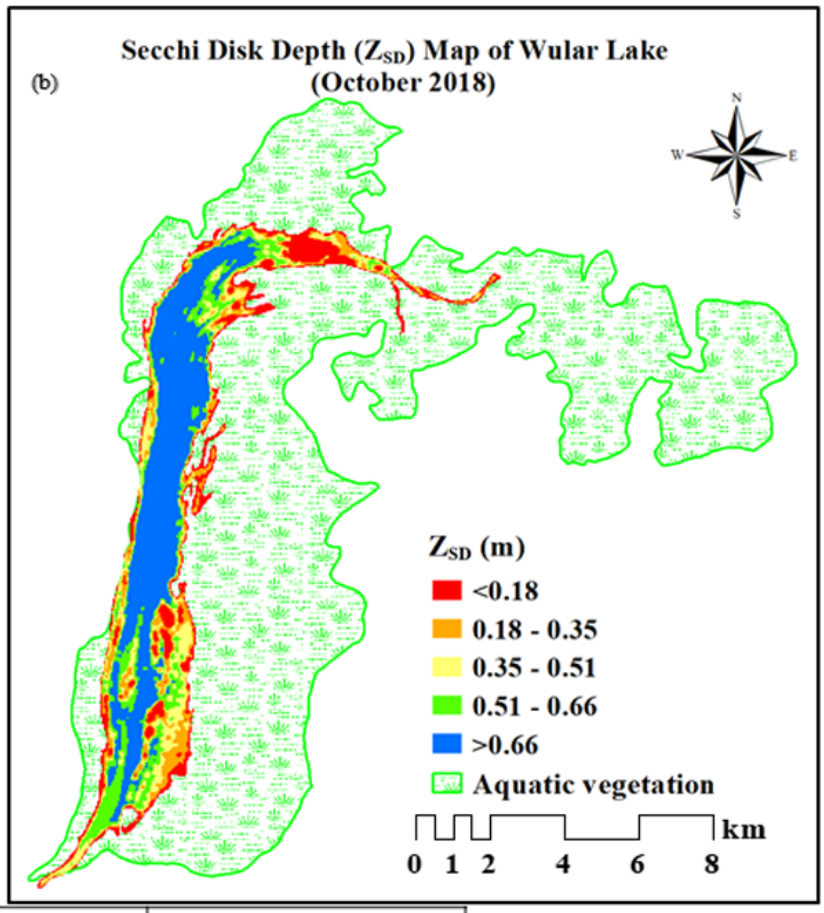

Descriptive statistics	C_{Chl-a} (µg/L)	Z_{SD} (m)
Minimum	1.79	0.02
Maximum	350.10	0.82
Mean	28.71	0.50

Figure 7.

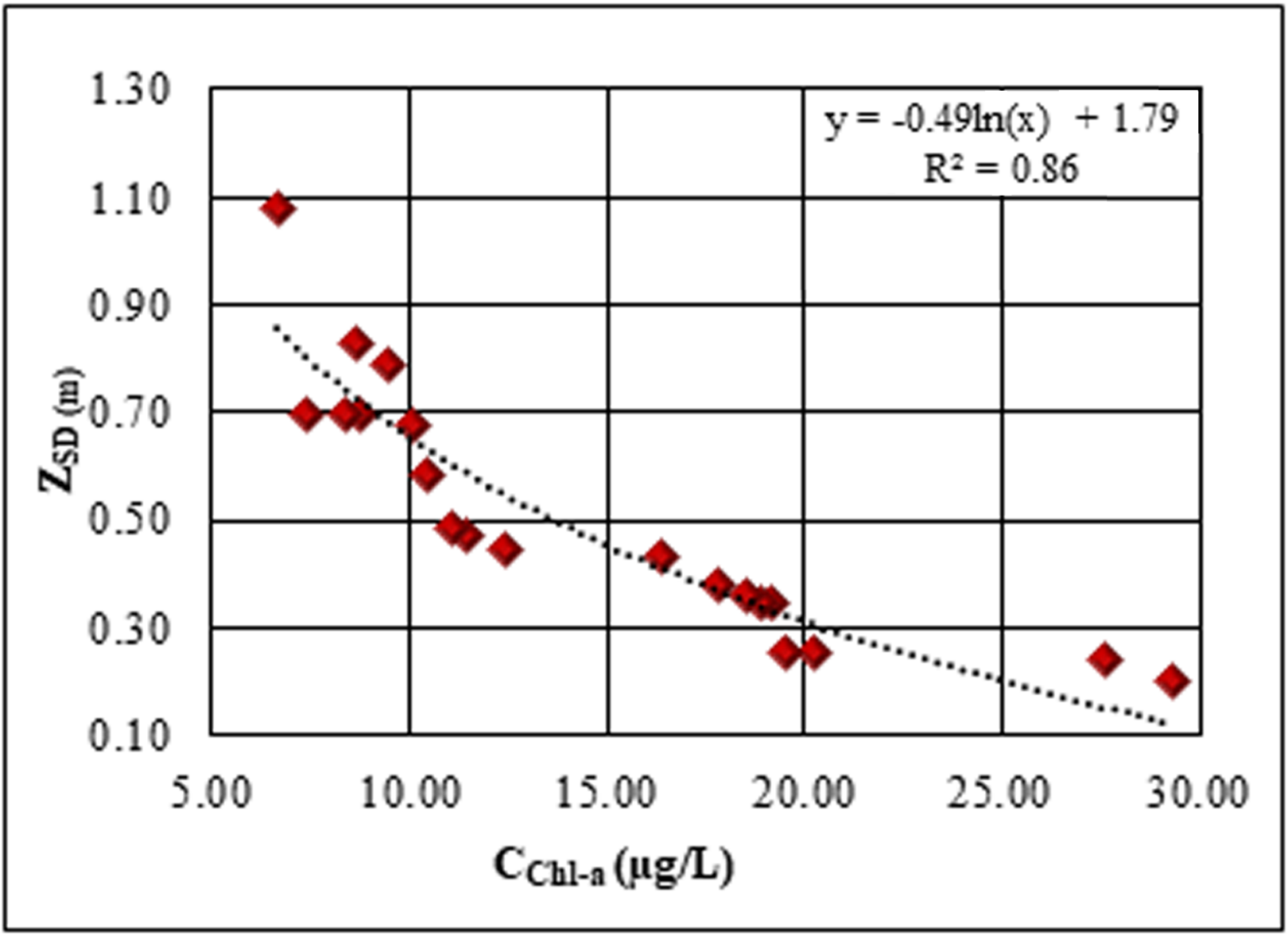
y = -0.49ln(x) + 1.79
R² = 0.86
1.30
1.10
0.90
0.70
0.50
0.30
0.10
Z_SD (m)
5.00
10.00
15.00
20.00
25.00
30.00
C_Chl-a (µg/L)

Figure 8.

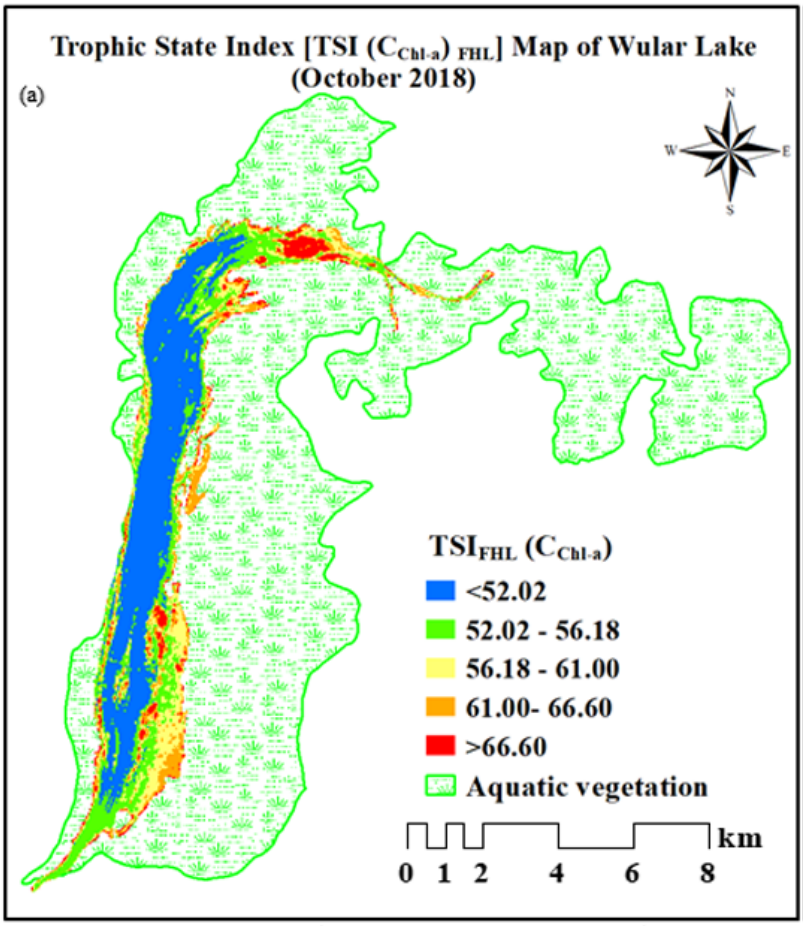

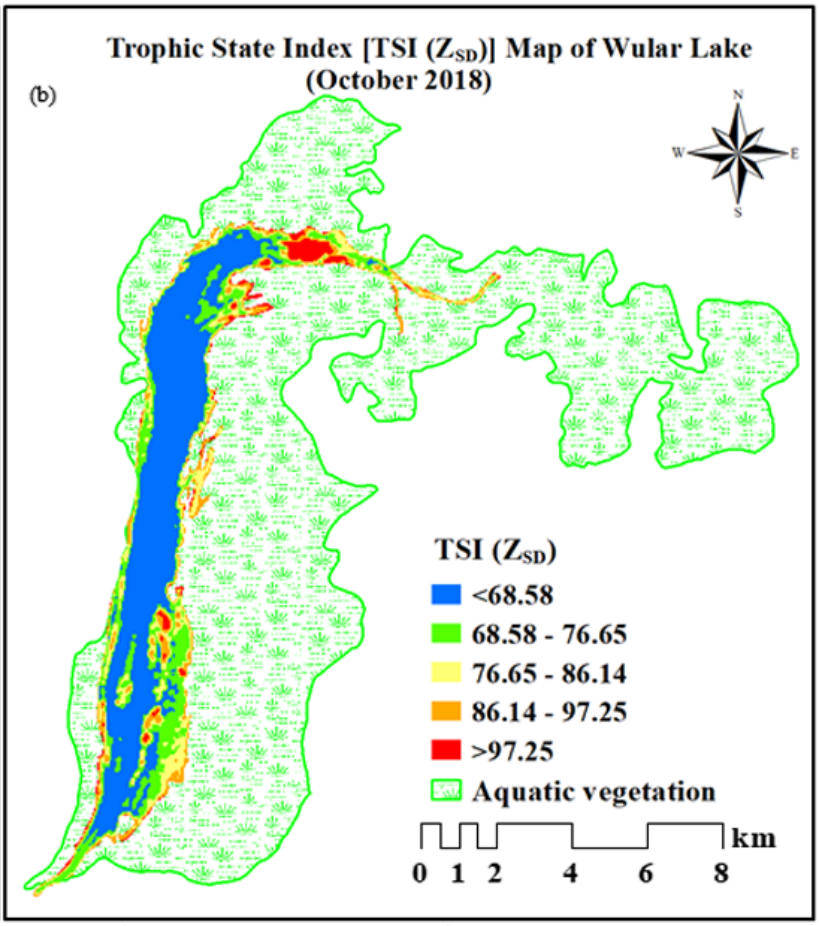

Descriptive statistics	TSI (C_{Chl-a})$_{FHL}$	TSI (Z_{SD})
Minimum	42.76	62.93
Maximum	75.96	114.41
Mean	55.03	72.78

Tables

Table 1 Geographic location of sampling sites, Secchi disk depth (Z_{SD}) and Chlorophyll-a Concentration ($C_{Chl\text{-}a}$) during October 2018 with descriptive metrics: minimum value (Min), maximum value (Max), and Mean values.

Sample Site	Latitude (N)	Longitude (E)	Elevation (m)	In-situ Secchi Disk Depth (Z_{SD}) (m)	Lab measured Chlorophyll-a ($C_{Chl\text{-}a}$) (µg/L)
S_1	34.37	74.54	1568.76	0.20	29.30
S_2	34.37	74.54	1573.34	0.25	20.21
S_3	34.37	74.54	1569.64	0.43	16.38
S_4	34.37	74.54	1576.63	0.34	19.20
S_5	34.37	74.54	1574.31	0.25	19.53
S_6	34.35	74.53	1572.99	0.34	18.86
S_7	34.34	74.54	1574.56	0.44	12.46
S_8	34.33	74.54	1568.27	0.38	17.85
S_9	34.32	74.53	1587.77	0.58	10.44
S_{10}	34.32	74.53	1575.24	0.47	11.45
S_{11}	34.31	74.53	1573.67	0.70	8.76
S_{12}	34.31	74.53	1572.79	0.70	7.41
S_{13}	34.30	74.53	1579.08	0.36	18.52
S_{14}	34.30	74.53	1576.78	0.67	10.10
S_{15}	34.30	74.53	1580.31	0.70	8.42
S_{16}	34.30	74.52	1575.48	0.79	9.43
S_{17}	34.29	74.52	1582.98	0.83	8.69
S_{18}	34.30	74.52	1581.37	1.08	6.66
S_{19}	34.29	74.51	1586.25	0.48	11.11
S_{20}	34.29	74.52	1584.59	0.24	27.62
Descriptive metrics				Min= 0.20 Max= 1.08 Mean= 0.51	Min= 6.66 Max= 29.30 Mean= 14.62

Table 2 Results of regression modelling presents the empirical correlation between sensor reflectance (L8 OLI) and biophysical parameters (chlorophyll-a concentration ($C_{Chl\text{-}a}$) and Secchi disk depth (Z_{SD})).

Bands/ Band combinations		Model equation		R^2	
$C_{Chl\text{-}a}$	Z_{SD}	$C_{Chl\text{-}a}$	Z_{SD}	$C_{Chl\text{-}a}$	Z_{SD}
ρw (865)	ρw (865)	$y = 720.95x - 85.96$	$y = 17.32e^{-24.33x}$	0.88	0.82
ρw (865) / ρw (655)	ρw^{-1} (865)	$y = 80.07x - 48.90$	$y = 0.01e^{0.57x}$	0.77	0.84
ρw (865) / ρw (561)	ρw (561) / ρw (865)	$y = 104.92x - 58.80$	$y = 0.02e^{2.42x}$	0.86	0.83
ρw (865) / ρw (482)	ρw (655) / ρw (865)	$y = 128.66x - 68.92$	$y = 0.02e^{2.53x}$	0.88	0.75
[ρw (865) - ρw (482)] / [ρw (865) + ρw (482)]	[ρw^{-1} (482)/ ρw^{-1} (865)]	$y = 178.01x + 52.65$	$y = 11.04e^{-4.53x}$	0.88	0.82
[ρw (865) - ρw (655) / ρw (655)]	[ρw^{-1} (561)/ ρw^{-1} (865)]	$y = 80.07x + 31.17$	$y = 9.52e^{-3.98x}$	0.77	0.81
[ρw (865) - ρw (482) / ρw (561)]	[ρw (482) - ρw (865)]	$y = 126.27x + 62.24$	$y = 0.07x + 0.03$	0.89	0.67
[ρw (865) - ρw (655)] / [ρw (865) + ρw (655)]	[ρw (561) - ρw (865)]	$y = 135.33x + 30.50$	$y = 0.07x + 0.01$	0.78	0.65
[ρw (865) - ρw (561)] / [ρw (865) + ρw (561)]	[ρw^{-1} (482)/ ρw^{-1} (865)] × [ρw^{-1} (561)/ ρw^{-1} (865)]	$y = 155.58x + 42.31$	$y = 2.10e^{-2.79x}$	0.86	0.80
[ρw (865) - ρw (482) + ρw (561)]	[ρw (482) / ρw (865) + ρw (561) / ρw (865) + ρw (655) / ρw (865)]	$y = 808.10x - 85.89$	$y = 0.02e^{0.82x}$	0.84	0.82

Table 3 Performance of selected best fit linear chlorophyll-a concentration ($C_{Chl\text{-}a}$) and exponential Secchi disk depth (Z_{SD}) regression algorithms with evaluated model errors.

Parameter	Band/Band ratio	Best-fit model	Error estimation		
			SEE	MAPE	*NSE*
$C_{Chl\text{-}a}$	[ρw (865) - ρw (482) / ρw (561)]	y = 126.27x + 62.24	0.77	5.83	0.98
Z_{SD}	[ρw^{-1} (865)]	$y = 0.01e^{0.57x}$	0.11	13.93	0.77

Table 4 Lake trophic state classification criteria as per (Aizaki et al., 1981; Carlson, 1977; Carlson & Simpson, 1996; Vollenweider & Kerekes, 1982) and correspondence to the, chlorophyll-a concentration ($C_{Chl\text{-}a}$) and exponential Secchi disk depth (Z_{SD}) parameters.

Trophic state category	Carlson, (1977); Carlson & Simpson, (1996)			Aizaki et al., (1981)		Vollenweider & Kerekes, (1982)	Characteristics
	TSI Range	$C_{Chl\text{-}a}$ (µg/L)	Z_{SD} (m)	$C_{Chl\text{-}a}$ (µg/L)	Z_{SD} (m)	$C_{Chl\text{-}a}$ (µg/L)	
Oligotrophic	<30	<2.6	>4	<1.6	>8	0.8-2.1	Classic Oligotrophy; Clear water, oxygen through the year in the hypolimnion.
Mesotrophic	30-50	2.6-6.4	4-2	1.6-10	8-2.5	2.2-6.3	Deeper lakes still exhibit classical oligotrophy, but some shallower lakes will become anoxic in the hypolimnion during the summer
Eutrophic	50-70	6.4-56	2-0.5	10-64	2.5-0.80	6.4-19.2	Dominance of blue-green algae, algal scums probable, extensive macrophyte problems.
Hypereutrophic	70-80	56-154	0.5-0.25	64-160	0.80-0.44	≥ 19.3	Heavy algal blooms possible throughout the summer, dense macrophyte beds, but extent limited by light penetration. Often would be classified as hypereutrophic
Extremely hypereutrophic	>80	>154	<0.25	>160	<0.44	-	Algal scums, summer fish kills, few macrophytes.

Table 5 The evaluation standards of the trophic state index for Freshwater Himalayan lake (TSI_{FHL}), derived from chlorophyll-a concentration (C_{Chl-a}).

Trophic state classification	TSI_{FHL}	C_{Chl-a} (μg/L)	Z_{SD} (m)
Oligotrophic	≤42	≤1.79	≥0.66
Mesotrophic	42-51	1.79-25.81	0.51-0.66
Light Eutrophic	51-56	25.81-61.69	0.35-0.51
Medium Eutrophic	56-61	61.69-115.51	0.18-0.35
Hypereutrophic	61-66	115.51-207.96	0.02-0.18
Extremely hypereutrophic	≥66	≥207.96	≤0.02